New insights into mechanisms of sunlight- and dark-mediated high-temperature accelerated diurnal production-degradation of fluorescent DOM in lake waters

New insights into mechanisms of sunlight- and dark-mediated high-temperature accelerated diurnal production-degradation of fluorescent DOM in lake waters

by

Yijun Liu[1,2], Jie Yuan[3], Fu-Jun Yue[1,2], Si-Liang Li[1,2], Baoli Wang[1,2], Mohammad Mohinuzzaman[1,2], Xuemei Yang[1,2], Nicola Senesi[4], Xinyu Lao[1,2], Longlong Li[1,2], Cong-Qiang Liu[1,2], Rob M. Ellam[5,1], Davide Vione[6], and Khan M.G. Mostofa[*1,2],

[1]Institute of Surface-Earth System Science, Tianjin University, 92 Weijin Road, Tianjin 300072, China.

[2]Tianjin Key Laboratory of Earth Critical Zone Science and Sustainable Development in Bohai Rim, Tianjin University, 92 Weijin Road, Tianjin 300072, China.

[3]Key Laboratory of Earth and Planetary Physics, Institute of Geology and Geophysics, Chinese Academy of Sciences, Beitucheng Western Road, Chaoyang District-100029, Beijing, PR China.

[4]Dip.to di Scienze del Suolo, della Pianta e degli Alimenti, Università degli Studi di Bari "Aldo Moro", Via G. Amendola 165/A, 70126 BARI –Italy.

[5]Scottish Universities Environmental Research Centre, Rankine Avenue, Scottish Enterprise Technology Park, East Kilbride, G75 0QF, UK.

[6]Università degli Studi di Torino, Dipartimento di Chimica, Via P. Giuria 5, 10125 Torino, Italy and Centro Interdipartimentale NatRisk, Via Leonardo da Vinci 44, 10095 Grugliasco (TO), Italy.

[*]Corresponding author: Phone: +8618322560509. E-mail: mostofa@tju.edu.cn

Abstract

The production of fluorescent dissolved organic matter (FDOM) by phytoplankton and its subsequent degradation, both of which occur constantly under diurnal-day time sunlight and by night time dark-microbial respiration processes in the upper layer of sunlit surface waters, influence markedly several biogeochemical processes and functions in aquatic environments and can be feasibly related to global warming (GW). In this work sunlight-mediated high-temperature was shown to accelerate the production of FDOM, but also its complete disappearance over a 24-h diurnal period in July at the highest air and water temperatures (respectively, 41.1 and 33.5°C), differently from lower temperature months. Extracellular polymeric substances (EPS), an early-state DOM, were produced by phytoplankton in July in the early morning (6:00-9:00), then they were degraded into four FDOM components over midday (10:00-15:00), which was followed by simultaneous production and almost complete degradation of FDOM with reformation of EPS during the night (2:00-6:00). Such transformations occurred simultaneously with the fluctuating production of nutrients (NH_4^+, NO_3^-, NO_2^-, PO_4^{3-} and dissolved Si), dissolved organic carbon (DOC), dissolved organic nitrogen (DON) and the two isotopes ($\delta^{15}N$ and $\delta^{18}O$) of NO_3^-. It was estimated that complete degradation of FDOM in July took place alongside with mineralization of approximately 15% of the initial DOC, which showed a nighttime minimum (00:00) in comparison to a maximum at 13:00. The FDOM components identified by fluorescence excitation-emission matrix (EEM) spectroscopy combined with parallel factor (PARAFAC) analysis consisted of EPS, autochthonous humic-like substances (AHLS) of C- and M-types distinctly, a combined form of C- and M-types of AHLS, protein-like substances (PLS), newly-released PLS, tryptophan-like substances (TLS), tyrosine-

like substances (TYLS), a combined form of TYLS and phenylalanine-like substances (PALS), as well as their degradation products. Finally, stepwise degradation and production processes are synthesized in a pathway for FDOM components production and their subsequent transformation under different diurnal temperature conditions, which provided a broader paradigm for future impacts on GW-mediated DOM dynamics in lake water.

Keywords: Fluorescent dissolved organic matter (FDOM); sunlight-mediated processes; dark-mediated microbial processes; transformation of FDOM; water samples; closed lakes

Highlights

- EPS are produced from phytoplankton by light-induced high-temperature processes in the morning.
- Disintegration of EPS into four FDOM and their complete disappearance occur in 24-h.
- EPS follows humic-like and protein-like formation paths, until its mineralization.
- Transformations of FDOM are linked with changes of nutrients, DOC, DON and $\delta^{15}N$ plus $\delta^{18}O$ of NO_3^-.
- Rapid mineralization of FDOM is a useful sign to predict the potential impact of GW.

1. Introduction

Natural organic matter (NOM) is a key material in sustaining all biogeochemical processes and phenomena in ecosystems. NOM originates from two primary sources, *i.e*. plant materials in terrestrial ecosystems and phytoplankton in aquatic systems. Terrestrial NOM, including soil humic substances (humic acid and fulvic acid) (Tadini et al., 2017; Senesi and Loffredo, 1999), can produce dissolved organic matter (DOM) that partially runs-off into surrounding aquatic environments (Zark and Dittmar, 2018; Mostofa et al., 2019). Conversely, autochthonous aquatic DOM includes organic substances such as, for instance, extracellular polymeric substances (EPS), autochthonous humic-like substances (AHLS), protein-like substances (PLS), and aromatic amino acids of various nature (Shammi et al. 2017a, 2017b, 2017c; Guidi et al., 2016; Zhang et al., 2009; Mostofa et al. 2013; Yamashita and Tanoue, 2003). Note that EPS are considered an early-stage DOM, defined as 'dissolved organic substances newly-formed and not yet converted into individual organic components', which derive from phytoplankton in surface water (Shammi et al. 2017a, 2017c; Sheng and Yu, 2006; Guidi et al., 2016; Zhang et al., 2009; Mostofa et al., 2013; Casareto et al., 2012). These substances occur as major DOM fractions, even if very diluted, in surface waters of lakes, estuaries and oceans, where they control many important aquatic biogeochemical functions and processes, including cycling of organic and inorganic carbon (C) (Zark and Dittmar, 2018; Guidi et al., 2016; Amon and Benner, 1994; Wang et al., 2020), nitrogen (N) (Yue et al., 2018; Liang et al. 2019), phosphorus (P) (Guidi et al., 2016; Carpenter et al., 1998; Parsons et al., 2017) and trace elements (Wan et al., 2019; Helms et al., 2013), as well as nutrient changes associated with diurnal sunlight-induced planktonic photosynthesis (Gao et al., 2010; Jung et al., 2013; Segschneider and Bendtsen., 2013).

Most key DOM components from both terrestrial and aquatic autochthonous sources display fluorescence properties, thus they are termed fluorescent DOM (FDOM) and can be studied in detail by fluorescence (excitation-emission matrix, EEM) spectroscopy combined with parallel factor (PARAFAC) analysis (Mostofa et al., 2019; Coble, 2007; Stedmon et al., 2003; Coble, 1996). Moreover, EEM-PARAFAC can be effectively applied in other studies such as fluorescent substances (e.g. humic-like, protein-like) in membrane bioreactors as well as metal-FDOM interactions (Cui et al., 2020; Sun et al., 2018; Cai et al., 2017). Key DOM components

include terrestrial humic substances (fulvic and humic acids), EPS, and aromatic amino acids (Coble, 1996; Yamashina and Tanoue, 2003; Yamashina and Tanoue, 2004; Shammi et al. 2017a, 2017b, 2017c; Zhang et al., 2009). Natural sunlight is the key driving force for the production of DOM and FDOM components by photosynthesis (Gao et al., 2010; Segschneider and Bendtsen., 2013), and for their photoinduced degradation in sunlit surface water (Moran et al., 2000; Cory et al., 2007; Mostofa et al., 2007; Hansen et al., 2016; Stedmon et al., 2007; Ward et al., 2013). These and subsequent processes typically convert high molecular weight (HMW) DOM into low molecular weight (LMW) DOM by producing hydroxyl radical ($^{\bullet}OH$) from either the photo-Fenton reaction or direct dissociation of H_2O_2 in sunlit surface waters (Vione et al., 2006; Catalán et al., 2016; Mostofa and Sakugawa, 2009; Mostofa and Sakugawa, 2016; Zhu and Kieber, 2018; Gligorovski et al., 2015). The action of microorganisms represents another key microbial degradation process that can alter DOM composition at night, *i.e*. in the absence of sunlight in both surface and deep water layers as well as soils (Amon and Benner, 1994; Moran et al., 2000; Hansen et al., 2016; Diaz et al., 2013; Amon and Benner, 1996; Mostofa et al., 2005; Ma and Green, 2004; Ye et al., 2019).

The global warming (GW) phenomenon is ascertained to cause an increase of ambient temperature as well as an extension of the summer season (Huisman et al., 2006). These changes are expected to induce greater water stratification with major potential implications for aquatic environments (Watanabe et al., 2011; Hoegh-Guldberg et al. 2019; Rogelj et al., 2019; Marañón et al., 2018). Although the Paris climate agreement has set Intended Nationally Determined Contributions designed collectively to lower greenhouse gas emissions, a median warming of 2.6–3.1°C is expected by 2100 (Rogelj et al., 2016). The GW effect appears to lead to more frequent and intense heat waves that are predicted to increase the minimum mortality temperature (Qian et al., 2019). GW is also associated with the risk of severe and, in some cases, irreversible impacts on ecosystems (Pachauri et al., 2014; Wernberg, 2016; Frölicher et al., 2018). The frequency of sunlight-mediated high temperatures, which is clearly interconnected with the effects of GW in increasing the overall ambient temperature, is reasonably expected to accelerate DOM degradation, as it does with most photochemical, microbial and physical processes in aquatic environments (Segschneider and Bendtsen., 2013).

Diurnal day-time (sunlight) and night-time (microbial) degradation processes are a natural phenomenon that depends on the photosynthetic activity of primary producers in surface waters, which is ultimately related to the daily biogeochemical changes of C, N and P cycling (Guidi et al., 2016; Segschneider and Bendtsen., 2013; Huisman et al., 2006; Carpenter et al., 1998). This overall day-night degradation of FDOM is caused by diurnal photo-microbial transformations. Photoinduced degradation of FDOM is usually observed in the euphotic zone, especially in the summer season (Mostofa et al., 2005; Borisover et al., 2009),), with a significant decrease with increasing water depth. Between the years 2006 and 2015 the ambient air mean temperature has increased by about 0.94 °C in Northwest China and 1.59 °C in Northeast-North China, compared to GW values estimated at 1.5-2.0 °C (Qian et al., 2019). Currently, it is still uncertain how increasing temperature-driven trends may impact the diurnal photo-microbial transformation of FDOM in freshwater lakes under GW scenarios. In any case, it is difficult to assess the potential impact of sunlight-mediated high-temperature on DOM dynamics due to the complexity of the various environmental parameters acting together.

The aim of this work was to investigate the diurnal daytime-photoinduced production of FDOM components and their associated cascade night-time-microbial degradation processes, as affected by temperature in two closed lake systems. Another aim of this study was to assess the variation of nutrient contents related to the production-degradation processes of FDOM, occurring during the diurnal cycles under different temperature conditions. Further, the diurnal transformation mechanisms of FDOM compositions are comprehensively discussed on the basis of the obtained results, which could be useful to predict future potential GW impacts.

2. Materials

Jingye lake and Qingnian lake are closed lakes with a watershed area of approximately 29568 m^2 and 45156 m^2, respectively, both located inside the campus of Tianjin University, Tianjin, China (39°6' N, 117°10' E) (Fig. S1). The water surface area of Jingye Lake is 29,068 m^2, the average depth is 3.6 m, and the total water volume is approximately 104,654 m^3. The water area of Qingnian Lake is the same as the watershed area (45,156 m^2), the average depth is 6.8 m and the total water volume is 30,7061 m^3. These lakes have always been existing since the foundation of the university and in 1980, the university authority decided to preserve all lakes in

the university. The lake water is not influenced externally, so as to preserve the water resources as natural ways and it is strictly forbidden to take bath in lakes. There is no connecting inflowing and outflowing channel to or from each lake, and rainwater is the most important water source. Jingye lake water is used by means of a pump to display artificial stream-flow and water-channels nearby Beiyang (Tianjin University) square, during the important events of the university. Therefore, water mobility is relatively better in Jingye lake than in Qingnian. All shore lines of the two lake basins are reinforced with granite, to prevent soil erosion from the surrounding terrestrial environment and for aesthetic reasons. Natural sunlight directly reaches the surface water of Jingye lake, due to the relatively lower presence of big trees or buildings around the lake basin. Differently, lesser sunlight can reach the surface water of Qingnian lake due to the presence of many big trees and buildings along the lake basin. Small aquatic plants and sea grasses are found to grow in the shallows along the lake shore in both lakes.

These two lakes are located in a typical warm-temperate semi-humid monsoon climate, and they are largely affected by the monsoon climate. Climate in winter is mainly controlled by the cold high pressure of Mongolia and in summer, it is mainly controlled by the heat and low pressure of the lower western Pacific. The annual air temperature varies from −18.1 to 40.5°C, with the hottest month in July and the coldest month in January according to Tianjin Meteorological Bureau website data for the last 10 years (http://www.nmc.cn/publish/forecast/ATJ/tianjin.html). Four seasonal timescales in Tianjin are apparently accounted for by winter (Nov–Mar, the longest season), spring (April–early May), summer (May–early Sept), and autumn (Sept–Oct). The annual precipitation was greatly variable from 355 to 755 mm in the last 10 years, and precipitation time is unevenly distributed throughout the year, with highest precipitation during the period from July to October.

Based on the earlier experiences on photodegradation of the upper sunlit layer and water column (Mostofa et al., 2005; Fu et al., 2010), to achieve monitoring objectives the diurnal sampling was designed to collect water from the uppermost surface layer, ~0-10 cm depth, using a clean plastic open container with a handle that is well connected with a rope. The container was washed three times before collecting each sample. Lake-water samples from Jingye lake were collected on July 5th and 6th, 2018, every hour over 24 h, whereas on October 12th and 13th, 2018, samples were collected every hour in day-time (6:00 – 18:00) and at two-hour intervals in night-

time (20:00 – 6:00). All times are expressed as Chinese Standard Time (CST). Diurnal sampling every hour over 24 h or at two-hour interval is extremely laborious as far as sample collection and simultaneous measurements are concerned. To overcome this situation, we have then planned to collect samples only twice-a-day: early morning (before sunrise) and in the afternoon (14:00), which could represent the overall nighttime microbial effect and day-time photochemical effects, respectively. For this reason on May 2nd and June 30th, 2019 we have collected water samples from the two lakes (Jingye and Qingnian) only twice-a-day, i.e. in the afternoon (14:00) and the early morning (6:00). For collecting the diurnal samples in Jingye lake, we have chosen the southern part (sunshine-exposed) of Truth-Seeking (Qiushi in Chinese) Memorial Tower that is built ~10 m inside the lake water with a bridge connecting it to the lake shore, whereas the tower base is very close to the water level (just 1 m or less). For Qingnian lake, we have carried out sampling in the western part that is best exposed to sunlight. Water samples from both lakes were collected also on one day in September 19th (2017), December 6th (2017), April 7th (2018) and June 5th (2018), covering four seasons (autumn, winter, spring and summer, respectively). For seasonal samples, we have collected from Truth-Seeking (Qiushi in Chinese) Memorial Tower, north side (east part), north side (west part) and west side of the lakes whilst for Qingnian lake, we have collected west, north, east and south sides. To understand the field-level accurate temperature variation, which is relevant to the effects of GW, water and air temperatures (WT and AT, respectively) were continuously measured at 10-min intervals using a sensor-based probe thermometer at the sampling site.

To elucidate the diurnal production and subsequent degradation of FDOM and compare day-time-sunlight effects to night-time-microbial implications, samples were grouped into five sub-diurnal samples, i.e. samples collected at: (a) early morning (6:00-9:00) subjected to relatively low sunlight irradiance; (b) mid-day (10:00-15:00) subjected to strong irradiance; (c) afternoon (16:00-20:00) subjected to moderate irradiance; (d) early-night (21:00-1:00) affected by mild microbial effects ; and (e) late night-early morning (2:00-6:00) affected by strong microbial activity. Based on selective characteristic samples (Mostofa et al. 2019), the PARAFAC model was applied individually to each of the five sub-diurnal water sample groups collected in the months of July and October. The number of water samples in each group were, respectively for July and October: 12 + 12 for early morning, 18 + 18 for mid-day, 15+15 for afternoon,15 + 6 for early night, and 15 + 9 for late night-early morning.

The samples were collected in 500 mL brown-glass bottles previously cleaned by submergence in HCl solution for 48h, and subsequently rinsed first with deionized water and then three times with ultra-pure water. Finally, the water samples were filtered through 0.45-μm glass-fiber filters (GF/F, Shanghai Xin Ya Purification Equipment Co. Ltd) which had been previously cleaned by burning for 5-h at 450 ℃ in an oven. We then measured fluorescence and absorbance after sample collection at the same time. For other parameters, filtered samples were stored in a refrigerator at 4°C and measured within 72h.

3. Methods

The DOC concentration was measured in triplicate on each sample using a total organic carbon (TOC) analyzer (OI Analytical Aurora, Model 1030W+1088, USA). A UV-VIS spectrophotometer (UV-2700, Shimadzu) was used to estimate the absorption properties of chromophoric DOM (CDOM). Ultra-pure water was simultaneously used in the reference cell as a blank. Concentrations of total N (TN), NO_3^-, NO_2^-, NH_4^+, PO_4^{3-} and dissolved silicon (DSi) were measured colorimetrically using an automated continuous flow analyzer (Skalar San++ System, Skalar Analytical B.V., The Netherlands) (Yang et al., 2020). Dissolved organic nitrogen (DON) was estimated by subtraction of NO_3^-, NO_2^- and NH_4^+ contents from the TN content. The pH and electrical conductivity (EC) were measured in the field in real time using a multi-parameter analyzer (YSL-EXO, YSI Company, USA). The isotopes $\delta^{15}N$ and $\delta^{18}O$ of NO_3^- in water samples were measured by a method described previously (Yue et al., 2018; Mcilvin and Casciotti, 2011) using four international NO_3^- standards, i.e. USGS-32, USGS-34, USGS-35 and IAEA-N3 (United States Geological Survey (USGS), USA *via* China Isotope & Radiation Corporation, Beijing, China), for calibration.

Samples of approximately 400 mL volume each were collected in 500 mL brown glass bottles at each time, to take microscopic images of phytoplankton. To stop the growth of phytoplankton, 1.5 mL 10% formaldehyde solution was added to each water sample. After standing for 36 h, the water sample was concentrated to 40 mL for night samples, and to 25 mL for day-time samples. To identify the phytoplankton species, microscopic images of phytoplankton at 40×10 magnification were obtained by the intelligent identification and counting instrument for algae (Algacount S300-3614025) (Hu and Wei, 2006). The solar intensity (SI) data were provided by

Tianjin Meteorological Agency, Tianjin, China, whereas WT and AT were measured at 10-min intervals using a sensor-based probe thermometer (Testo 175 Q/DT01, China).

Fluorescence EEM spectra were recorded with a fluorescence spectrophotometer (F-7000, Hitachi, Japan) according to procedures reported elsewhere (Mostofa et al., 2010). The scanning ranges were 220–400 nm for excitation at intervals of 5 nm and 280–500 nm for emission at intervals of 1 nm using a scanning speed of 1200 nm min^{-1} and a photomultiplier voltage of 700 V. The slit width for both excitation and emission was set at 5 nm and all EEM spectra were recorded in both excitation and emission corrected mode. Ultrapure water (18.2 MΩ.cm) was used as the blank and measured before sample analysis after every 10 samples. In some cases, water samples were diluted to avoid inner filter effects (IFE), after which the most commonly used absorbance-based approaches (Kothawala et al., 2013; Lakowicz, 2018) were applied to correct IFE in EEM measurements.

In this work PARAFAC analysis was performed using the "N-way Toolbox for MATLAB" (Andersson and Bro., 2000). Before applying PARAFAC, EEM data were preprocessed by subtracting Rayleigh and Raman peaks measured on a ultrapure water blank from experimental EEM spectra, using a home-made Excel Program (Shammi et al. 2017a, 2017c; Mostofa et al., 2010). Finally, non-negative constraints were applied to the PARAFAC model. Further, to avoid the possible production of artifacts by mixing of fluorescent components among different water samples (Mostofa et al., 2010), PARAFAC analysis was performed on selective characteristic samples (Mostofa et al., 2019). The detailed procedure followed in applying PARAFAC modeling to EEM spectra is described in the supplementary information.

4. Results and Discussion

4.1. Diurnal features of FDOM in Jingye and Qingnian lake waters

4.1.1. Water samples collected in July from Jingye lake

The EEM-PARAFAC results that are shown in Table 1 and Fig. 1 suggest that the fluorescent components in water samples collected from Jingye lake in the early morning of July 5th and 6th were similar and consisted of EPS in a combined form of PLS, showing two fluorescence peaks (T at 270/365 nm and T_{UV} at 230/365 nm; hereinafter these are the

excitation/emission wavelengths) and M-type AHLS, also showing two fluorescence peaks (M at 270/394 nm and A at 230/394 nm). EPS derive from phytoplankton by microbial activity under dark late-night early-morning conditions at relatively high WT (29.2-29.9 °C) and low AT (25.4-26.2 °C) (Figs. 2, S2). The EPS excreted from microorganisms were shown to be composed mainly of polysaccharides, proteins, nucleic acids, lipids and a HMW mixture of polymeric AHLS (Yu, 2020; Flemming and Wingender, 2010; Jenkinson and Lappin-Scott, 2011). Apparently, EPS generated in the early morning were subsequently degraded during mid-day time (10:00-15:00) into four FDOM components that include: (a, b) AHLS of C- and M-types featuring two fluorescence peaks each, i.e., respectively C at 315/418 nm and A at 260/418 nm, as well as M at 305/383 nm and A at 220/383 nm; (c) TLS showing two fluorescence peaks (T at 270/338 nm and T_{UV} at 225/338 nm); and (d) newly-released PLS featuring two fluorescence peaks (C at 315/418 nm and A at 260/418 nm) (Table 1, Fig. 1). FDOM production upon degradation of EPS would occur during the gradual increase of solar irradiance (SI, from 1.36 to 2.97 MJ/m^2 for a total of 15.26 MJ/m^2), at a WT of 30.2-33.7 °C and AT of 35.4-41.8 °C (Fig. 2).

In the late-afternoon early-evening time period (16:00-20:00), a number of changes in the four FDOM components occurred (Table 1, Fig. 1) under the varied conditions of SI (from 0.01 to 0.85 MJ/m^2 for a total of 1.77 MJ/m^2), WT (30.9-33.4 °C) and AT (29.0-38.1 °C) (Fig. 2). In particular: (a) newly-released PLS with a peak T at 280/351 nm appeared and the T_{UV} peak disappeared, whereas (b) the intensity of the peak T of newly-released PLS increased by 49%; (c) the fluorescence peak C of C-type AHLS was partly shifted to longer wavelength, i.e. 325/430 nm; (d) peak M of M–type AHLS showed a 3.2-fold intensity increase; and (e) the fluorescence intensity of peak C of C-type AHLS and of peak T of TLS decreased, respectively, by about 3% and 63%. It is well-known that the daytime-photoinduced degradation of FDOM could be ascribed to the occurrence of the photo-Fenton reaction, which produces the strong oxidizing agent $^{\bullet}$OH radical by interaction of H_2O_2 and Fe^{2+} in the presence of sunlight (Vione et al., 2006; Mostofa and Sakugawa, 2016; Gligorovski et al., 2015). In the early-night samples, with 29.9-30.8 °C WT and 26.0-28.9 °C AT (Fig. 2), only two FDOM components, i.e. AHLS of C-type and TLS were identified. Their intensity was increased by, respectively, ~40% and 3.2-fold, whereas the other two fluorescent components disappeared completely.

Finally, in the samples collected during late-night early-morning (2:00-6:00) under conditions of 29.2-29.9 °C WT and 25.4-26.2 °C AT (Fig. 2), only EPS generated from grazing/respiration of primary producers, i.e. phytoplankton were identified, whereas the other fluorescent components disappeared completely. In particular, the fluorescence intensity of EPS in this time period was approximately 3% lower than in the early morning, as shown by the microscope images of phytoplankton that mostly disappeared during the day (Fig. S2). The diurnal changes of FDOM components could be reasonably caused by: (a) the simultaneous photoinduced production and microbial degradation of FDOM under daytime conditions of high sunlight intensity and ambient temperature, as also reported by previous *in situ* experimental investigations (Moran et al., 2000; Mostofa et al., 2005, 2007; ; Ma and Green, 2004), and (b) night-time extended microbial degradation, which is also supported by the net decrease of DOC along with nutrients during the night, and will be comprehensively discussed in the next section. In summary, the July 2018 sampling campaign was performed at the highest AT (ranging from 25.4 to 41.8 °C with an average of 31.6 °C) and WT (ranging from 29.2 to 33.7 °C with an average of 31.0 °C) and a daily total solar intensity of 21.39 MJ m^{-2} (Fig. 2).

4.1.2. Water samples collected in October from Jingye lake

The diurnal transformations of samples collected in October under conditions of lower sunlight irradiation and lower WT and AT values were partially different from those collected in July. In October, four fluorescent components were identified in water samples collected in the early-morning (6:00-9:00) under conditions of SI ranging from 0.004 to 1.34 MJ/m^2 (for a total of 2.29 MJ/m^2), WT ranging from 16.5 to 18.3 °C, and AT from 9.4 to 14.5 °C (Fig. 2). These included AHLS of C- and M-types, PLS and degraded TLS (Table 1, Fig. 3). In particular, PLS were identified by two fluorescence peaks (T at 285/352 nm and T_{UV} at 235/352 nm), whereas the peaks of the other three FDOM components were similar to those of the July samples, although peak intensities varied depending on sunlight-driven temperature (Table 1, Fig. 3). In particular, newly-released PLS could be recognized by a major T peak and a minor T_{UV} peak, while TLS showed the typical peaks T_{UV} at 220-225 nm and T at 270-280 nm with an intensity ratio of 5.2, which is the key signature that distinguishes TLS from PLS.

In the subsequent mid-day temporal interval (10:00-16:00), characterized by SI ranging from 1.34 to 2.26 MJ/m^2 for a total of 11.46 MJ/m^2, WT from 18.1 to 20.6 °C and AT from 15.2 to

22.9 °C (Fig. 2), few variations of fluorescence peaks were detected for the four components (Table 1). The peak intensity ratio (T_{UV}/T) was 1.14 for PLS and 2.72 for TLS. Further, compared to early-morning samples, the fluorescence intensity increased by approximately 63% for peak M (HLS) and 58% for peak T (TLS). In contrast, it decreased by approximately 9% for peak C of AHLS and 5% for peak T of PLS.

The water sample collected in the afternoon-evening (16:00-20:00) under conditions of very low SI (from 0.14 to 0.57 MJ/m^2 for a total of 0.71 MJ/m^2), low WT (17.5-20.2 °C) and low AT (15.5-22.7 °C) showed three fluorescent components identical to those of the earlier phases, but the PLS peaks disappeared completely. The fluorescence intensity increased slightly, i.e. by approximately 9% for C-type AHLS and 4% for TLS, but it decreased by 16% for M-type AHLS. In the following early-night temporal period (21:00-1:00) under conditions of no sunlight and relatively low WT (16.8-17.4 °C) and AT (14.2-15.7 °C), four fluorescent components were identified of which three were identical to those detected in the samples of the previous periods and the fourth was ascribed to PLS newly-released from phytoplankton (Fig. 3). Further, fluorescence intensities decreased by approximately 23% for M-type AHLS and 4.6% for TLS, but they increased by about 31% for C-type AHLS. Lastly, in the late-night early-morning period (2:00-6:00) with no sunlight and low WT (14.0-16.8 °C) and AT (13.9-14.8 °C), four fluorescent components were identified, i.e. M-type AHLS freshly generated by the disappearance of newly-released PLS, a degraded M-type AHLS, C-type AHLS and TLS. Compared to the previous period the relevant fluorescence intensities decreased by, respectively, ~34%, 15% and 52% (Table 1, Fig. 3). The production of AHLS of M-type was the key signature of freshly formed DOM from newly-released PLS, produced in the previous time period. Apparently, in October, the low sunlight-affected ambient temperature was not able to degrade all FDOM in a 24-h cycle and, correspondingly, EPS was not generated from phytoplankton as it did in July. The newly released PLS generated in early-night time suggested their possible derivation from EPS, whereas their low concentration and rapid subsequent transformation into other FDOM components would support their absence in water samples collected in October.

4.1.3. Water samples collected in May and June from Jingye lake

The diurnal results measured on FDOM components in July and October samples showed that the most important changes occurred in the afternoon at around 14:00, due to day-time

sunlight-induced production and degradation, and in the early morning before sunrise (6:00), because of night-time microbial processes. Therefore, water samples in May and June were collected only twice-a-day, i.e. in the afternoon (14:00) and the early morning (6:00). Three FDOM components were identified in water samples collected in May at 14:00, after a 6:00-14:00 time interval under SI conditions of 20.47 MJ/m^2, WT from 19.2 to 26.9 °C with an average of 22.4 °C and AT from 17.1 to 35.3 °C with an average of 26.0 °C (Fig. 4). The identified components included AHLS of C- and M-types as well as TLS, the fluorescence wavelengths of which were similar to those previously described (Fig. 4; Table 2). Compared to samples collected at 6:00, the peak intensity increased for samples collected at 14:00 by approximately 36% for C-Type AHLS and by 14% for TLS, but decreased by 95% for M-Type AHLS. These results suggest that M-Type AHLS was degraded rapidly by sunlight-induced photoprocesses, whereas the other two FDOM components could regenerate from phytoplankton by photorespiration. The new production of C-Type AHLS was supported by the longer emission wavelength of peak C, i.e. 340/468 nm, measured at 14:00 with respect to that at 6:00, i.e. 340/449 nm (Table 2).

Also in June, three FDOM components were identified in the early morning (6:00) samples, i.e. AHLS of C- and M-types and TLS. In contrast, in the early afternoon samples (14:00), besides the typical C-type AHLS and TLS, a degraded EPS featuring four fluorescence peaks was detected (Fig. 5). It included a combined form of C- and M-types of AHLS, whose wavelengths were shifted to longer values than in July, with disappearance of any PLS contribution (Table 2, Fig. 5). The FDOM transformations described above occurred under conditions of SI of 21.18 MJ/m^2, with WT ranging from 27.5 to 33.9 °C with an average of 29.7 °C, and AT ranging from 24.7 to 39.9 °C with an average of 30.4 °C. Apparently, the overall night-time FDOM microbial production was altered in the early morning (6:00) with subsequent production of new FDOM components under strong day-time sunlight until 14:00. These three components identified in the early morning and afternoon samples of May and June in Jingye lake were observed in different diurnal timescales (Figs. 1, 3). They are also resembled with microbially-derived components from phytoplankton (Zhang et al. 2009), as well as sunlight-induced material released from EPS (Shammi et al., 2017a, 2017b). Thus, the increased sunlight-mediated ambient high-temperature that is expectedly experienced under GW conditions will probably accelerate FDOM production, as well as its transformation into LMW DOM within the

24-h period, as observed in July but not in lower temperature months. These results suggest that FDOM components in the early morning (6:00) and noon (14:00) of May and June do not degrade completely, differently from July diurnal samples because of low WT and AT, which could be useful indicators for daytime sunlight-induced and nighttime microbial degradation processes, respectively.

4.1.4. Water samples collected in May and June from Qingnian lake

Unlike Jingye lake, four fluorescent components were identified in May in Qingnian lake waters at both 6:00 and 14:00. They included C- and M-types of AHLS and TLS, as well as new components such as TYLS and PALS, which have been previously detected in surface waters (Yamashita and Tanoue, 2003; Shammi et al., 2017c; Zhang et al., 2009). In particular, partially degraded TYLS were detected at 6:00 featuring only one fluorescence peak (T_{UV} at 220/313 nm), whereas at 14:00 a combined form of TYLS and PALS with two fluorescence peaks (T at 255,265/321,306,310 nm and T_{UV} at 220/321 nm) was detected (Table 2, Fig. 5). The occurrence of peak T with two excitation maxima and three emission maxima suggests the existence of a combined state of TYLS and PALS that could originate from EPS. This state was detected for the first time in this work, thus adding new information on the sequential formation of two aromatic amino acids in a combined state under current lake environmental conditions. The fluorescence intensity of C-type AHLS remained almost constant (2% decrease), whereas those of M-type AHLS and TLS increased, respectively, by approximately 4% and 30% at 14:00 compared to the values measured at 6:00. The production and degradation processes of FDOM described above occurred at a SI of 20.47 MJ/m^2, a WT between 19.5 and 23.4 °C with an average of 21.5 °C, and AT between 17.6 and 38.7 °C with an average of 26.2 °C (Fig. 2).

Similarly, four FDOM components were identified in June at both 6:00 and 14:00, which included C- and M-types of AHLS, newly-released PLS (6:00) or PLS (14:00) and TLS (Table 2, Fig. 5). The newly-released PLS occurring in waters collected in the early morning (6:00) were identified by two fluorescence peaks, i.e. a major (in terms of fluorescence intensity) peak T at 290/346 nm, and a minor peak T_{UV} at 230/346 nm. Apparently, the newly-released PLS detected in the early morning (6:00) would be converted into different PLS detected at 14:00, which featured two fluorescence peaks (T at 285/340 nm and T_{UV} at 225/340 nm). During the 6:00 to 14:00 time period the fluorescence intensity of the C-type AHLS decreased by approximately

26%, whereas those of M-type AHLS and TLS increased, respectively, by 43% and 16%. These FDOM modifications occurred at a SI of 21.18 MJ/m^2, a WT between 26.9 and 36.8 °C with an average of 30.4 °C, and an AT between 23.6 and 41.5 °C with an average of 30.5 °C (Fig. 2). The detection of newly-released PLS in June in the early morning (6:00) was a key signature indicating a fresh input from EPS under conditions of enhanced WT, which could have occurred during the night due to microbial respiration. However, such scenarios were not observed in the same lake in May, when WT was significantly lower than in June (Fig. 2). With respect to May, the overall fluorescence intensity in June at 14:00 decreased by approximately 39% for C-type AHLS and 40% for TLS, but that of M-type AHLS increased by 47%. This finding suggests that FDOM production-degradation dynamics varied significantly, depending on sunlight-mediated ambient temperature.

4.1.5. Seasonal characteristics of FDOM and its transformation in the two lakes

The fluorescent components in Jingye lake water varied significantly between the four seasons (Table S1, Fig. S3). In particular, in autumn three FDOM components were identified including AHLS (C- and M-types) and PLS (Fig. S3), whereas four components were identified in the other three seasons, of which the first two were similar in all seasons. A third component was identified as newly-released PLS featuring two fluorescence peaks, a major one (T at 285/369 nm) and a minor one (T_{UV} at 250/369 nm) in samples collected in spring, but only one peak (T at 285/354 nm) in the summer sample. The fourth component was identified as TLS. These results suggest that C- and M-types AHLS were detected in all seasons, whereas the major changes in FDOM could be attributed to proteinaceous components, i.e. PLS and their transformation products, i.e. individual aromatic amino acids including TLS, TYLS and PALS.

The FDOM components in Qingnian lake waters also changed substantially as a function of the season. In detail: (a) two components, i.e. M-type AHLS and an unknown degraded component in autumn; (b) one component, i.e. EPS as a combined form of HLS and PLS with four fluorescence peaks, in winter; (c) two components, i.e. C-type AHLS and TLS in spring; and (d) four components, i.e. C- and M-types AHLS, newly-released PLS and TLS in summer (Table S1, Fig. S4). These results suggest that at low winter temperatures EPS could be produced in lake water, and that the seasonal production of FDOM and its biogeochemical transformations

differed between the two lakes, which could be ascribed to the different lake conditions and surrounding environmental factors.

4.2. Biogeochemical processes involving DOC and nutrients in lake Jingye

In July, the DOC concentration varied hourly from a minimum of 815 μM C achieved in the night (from 21:00 to 6:00) to a maximum of 963 μM C reached during the day (from 10:00 to 16:00), with a highest DOC fluctuation of 15% (Table S2, Fig. 6). In October, the DOC content was generally higher than in July and varied from low values with a minimum of 975 μM C in the early morning (6:00), to a maximum of 2989 μM C during day-time (10:00-15:00) with an increase of approximately three fold at 14:00 (Table S2, Fig. 6). The trends of DOC concentration were paralleled by those of nutrients, which in October were generally higher and more fluctuating along the day than in July (Table S2, Fig. 6). In particular, in July the NO_3^- content decreased by about 20% from the early morning (6:00-9:00) to middle day (10:00-15:00), and it subsequently increased (1.0-7.8%) in all successive sub-diurnal samples. In contrast, in October it increased by about 10% during the morning from 6:00 to 15:00, then remained nearly constant and increased again by about 16% during night time (2:00-6:00). Differently, NO_2^- increased substantially (70-94%) during day-time in October compared to July (0.5-14.4%), but then decreased significantly (5.0-5.8%) during night-time. This finding suggests a reasonably rapid turnover rate of NO_2^- during phytoplankton growth. Similarly, NH_4^+ substantially increased in October (117-257%) compared to the same time interval in July (4.1-41.7%), with the highest increase in the middle of the day (10:00-15:00). The DON content increased (7.6-31.0%) between 6:00-9:00 in July, whereas it was not detected in samples collected in October. The PO_4^{3-} content decreased significantly in July during the 16:00-20:00 period and then increased (18-34%) during the night, whereas in October it decreased (11-40%) in night-time, showing the highest concentrations in the 16:00-20:00 time period. In July, DSi decreased (3-17%) from the early morning (6:00-9:00) to late day, with an early night (21:00-1:00) increase by 23%. In contrast, DSi was absent in samples collected in October, which suggests its complete uptake by phytoplankton during the strong growth period occurring in this month.

The production of nutrients in October exceed that of July by a factor that was estimated to be approximately 16.0, 28, 4.0 and 23.8-fold higher for, respectively, NO_3^-, NO_2^-, NH_4^+, and PO_4^{3-} (Fig. 6). In particular, in October the highest NH_4^+ concentration paralleled the highest

DOC concentration detected at the same time (14:00) (Table S2, Fig. 6), which might suggest a rapid biogeochemical transformation of organic matter (e.g. phytoplankton) into DOC via FDOM and nutrients under ambient lake conditions. Apparently, the NH_4^+ formation in October was followed by subsequent rapid nitrification and denitrification (14:00) (Table S2, Fig. 6). Similarly, the lowest level of NH_4^+ at 10:00 was consistent with the lowest level of NO_3^-. Further, the occurrence of nitrification was confirmed by the decrease in NH_4^+ contents occurring simultaneously to the increase of NO_3^- in early morning samples (Table S2, Fig. 6).

Further evidence of the photosynthetic activity of phytoplankton was provided by the significant shifting of the $\delta^{15}N$ value of NO_3^-. In particular, in July the $\delta^{15}N$ value decreased from +0.67‰ at 10:00 to –0.02‰ at 12:00, which corresponded to an increase in SI from 2.33 MJ m^{-2} to 2.95 MJ m^{-2} (for a total of 8.14 MJ m^{-2}). In contrast, the $\delta^{18}O$ value of NO_3^- increased from +5.28‰ at 10:00 to +9.3‰ at 12:00 under conditions of elevated SI and high WT (36.5-39.9 °C) and AT (31.0-32.7 °C). The decrease of $\delta^{15}N$ and increase of $\delta^{18}O$ in NO_3^- with increasing SI from 10:00 to 12:00 suggest the uptake of lighter $\delta^{16}O$-containing NO_3^- by phytoplankton because of enhanced photosynthesis. This effect was confirmed by the 20% decrease of NO_3^- from 9:00 to 15:00 in July. In samples collected in October, the disappearance of DSi with the corresponding high production of DOC and nutrients would indicate the occurrence of high photosynthetic activity, together with both photoinduced processes and microbial respiration of planktonic organisms, which confirmed earlier results (Fan and Glibert, 2005; Guidi et al. 2016; Parsons et al. 2017; Condon et al. 2010; Carpenter et all. 1998; Elser et al. 1995). Thus, the activity of photosynthetic planktonic communities in sunlit surface water with the simultaneous release of DOC and nutrients could represent the driving force of the overall biogeochemical processes and functions occurring in surface lake waters.

4.3. An overall view of production and degradation pathways of FDOM in lake waters

As the different components of FDOM are related to one another, their sequential derivation/origin from phytoplankton and their subsequent transformation steps can be illustrated in the pathway shown in Fig. 7 and detailed in Figs. 8 and 9. In particular, in the first step primary DOM producers, mainly phytoplankton, generate EPS that in the second step produce FDOM components of various nature, which in the third step are subject to simultaneous or

subsequent stepwise degradation and production processes that follow two major distinct and parallel pathways. On the basis of results described and discussed above, these pathways can be reasonably hypothesized to consist of: (a) EPS transformation into a combined form of AHLS of C- and M-types, and their subsequent conversion into degraded forms that finally yield LMW DOM and mineralized end-products (Fig. 8), which are commonly detected in surface waters (Shammi et al. 2017a, 2017b, 2017c; Sheng and Yu, 2006; Sheng et al. 2010); and (b) EPS conversion into newly-released PLS that subsequently generate PLS and individual TLS, TYLS and PALS. The latter are finally degraded into LMW DOM and mineralized end-products (Fig. 9), which have been detected previously in surface water as well as in EPS exposed to sunlight (Mostofa et al., 2019; Zhang et al., 2009; Mostofa et al. 2013; Shammi et al. 2017a, 2017b; Yamashita and Tanoue, 2003; Mostofa et al. 2010). Further, in the last step as well as in all previous steps, mineralized end-products including nutrients, CO_2, dissolved inorganic carbon (DIC: dissolved CO_2, H_2CO_3, HCO_3^-, and CO_3^{2-}), H_2O_2, etc., are continuously produced under both diurnal sunlight-induced degradation and night-time microbial degradation. Note that Shammi et al. (2017a) have shown experimentally that EPS could firstly produce M-type AHLS, newly-released PLS and TYLS, and that all these components were subsequently degraded except for newly-released PLS. Correspondingly, DOC concentration (0 h: 308.97±1.2 mg L^{-1}; T = 22-30°C) decreased by 9.5% during the first six hours of irradiation and decreased by an overall 38.4% after 58 hours of irradiation in the same study. In another photoexperiment (time: 0-72 h and air temperature: 20-31°C), it has been shown that EPS can produce M-type AHLS, PLS and TYLS, of which the former two are subsequently degraded. At the same time, the DOC concentration (0-h: 103.5 ± 1 mg L^{-1}) decreased by approximately 6.9% within first six hours and after that it did not change any longer (Shammi et al., 2017b).

In more detail, the currently undefined formation of EPS in the first step of the process described above has been proven to occur mainly in July in the early-morning (from 6:00 to 9:00), which is indicative of EPS production under the effect of sunlight-induced, high-temperature, day-time microbial respiration. Moreover, the subsequent degradation into various FDOM components would occur under intense sunlight (from 10:00 to 15:00), followed by simultaneous production-degradation processes taking place under relatively less intense irradiance (from 16:00 to 20:00). Finally, FDOM is degraded almost completely during the night (from 21:00 to 6:00). In contrast, only partial transformation of FDOM components was

measured in water samples collected in the other months, due to lower solar intensity as well as water and air temperatures with respect to July. Although an accurate calculation of the net production-degradation of FDOM components is very difficult due to the simultaneous occurrence of these processes under either photo-respiration in day-time or microbial respiration in night-time, the net diurnal changes of fluorescence intensities calculated as a function of time, which have been discussed in detail in the previous section, can provide a good quantitative approximation of the processes under investigation.

4.4. Environmental implications and global warming

The complete degradation of FDOM after its formation from phytoplankton in July (Fig. 1) can be ascribed to the gradual increase in SI (from 1.36 to 2.97 MJ/m^2 for a total of 15.26 MJ/m^2) at the highest WT (30.2-33.7 °C) and AT values (35.4-41.8 °C) (Fig. 2). These environmental conditions are directly responsible for the rapid production of FDOM by phytoplankton, and for its corresponding rapid degradation by sunlight-induced and microbial processes. Such a complete sequential diurnal degradation of FDOM was not observed in October, May and June samples (Figs. 3-5), when solar intensity, AT and WT were relatively low compared to July samples (Fig. 2). In October, only one component (PLS) was completely mineralized in the 16:00-20:00 period among the four FDOM components detected in the five sub-diurnal samples (Figure 3). As discussed previously, the production and degradation of FDOM are related to simultaneous significant fluctuations in the contents of NO_3^-, NH_4^+, NO_2^-, DON, PO_4^{3-}, DSi and DOC (Fig. 6; Table S2). Photochemical and microbial processes can transform EPS into various forms of FDOM (Shammi et al., 2017a, 2017b) that are related to field observations, and show that different components of EPS vary over different timescales and temperatures (Shammi et al., 2017c; Sheng and Yu, 2006). Many studies provided evidence that photochemical and microbial degradation processes increase with increasing temperature and light intensity (Matsumoto et al., 2007; Weston and Joye, 2005; Malinverno and Martinez, 2015; Whelan and Rhew, 2015; McKay and Rosario-Ortiz, 2015; Grannas et al., 2006; Farias et al., 2007). In addition, DOC concentration reached its highest level (15% and three-fold increase compared to the 6:00-level in July and Oct, respectively) at noon time (13:00-14:00). Such an increase in DOC is significantly influenced by sunlight-induced photosynthetic activities, along with the simultaneous occurrence of photorespiration (Wan et al., 2015; Hagemann et al., 2016; Koller et

al., 2012; Perez-Garcia et al., 2011), photodegradation (Moran et al., 2000; Mostofa et al., 2007; Winter et al., 2007; Shammi et al., 2017a, 2017b) and photoinhibition depending on light intensity and temperature (Gao et al., 2008, 2010; Jiang and Qiu 2011; Bruhn and Gerard, 1996). Note that cyanobacteria or phytoplankton cells can utilize photosynthetically active radiation (PAR, 400–700 nm) to drive photosynthesis within the euphotic zone (Abboudi et al., 2009; Li et al., 2011; Cosby et al., 1984). Correspondingly, photorespiration could release organic substances and nutrients (e.g. NH_3) from photosynthetic organisms, which would occur mostly in the 11:00-15:00 time period (Beardall et al., 1989; Hull et al., 2008; Wan et al., 2015; Hagemann et al., 2016; Koller et al., 2012). At the same time, photodegradation could significantly decrease the DOC as is commonly observed in experimental studies (Moran et al., 2000; Mostofa et al., 2007; Winter et al., 2007; Shammi et al., 2017a, 2017b). Therefore, an increase in DOC during daytime could be decoupled by photorespiration, thereby providing a useful biogeochemical understanding of DOM dynamics in lake environments. In addition, photoinhibition could occur in the euphotic zone at high temperature >25-50°C, driven by solar intensity, thereby reducing cell growth and photosynthetic rates, damaging proteins or DNA molecules, pigments, and even leading to cell death (Gao et al., 2008, 2010; Jiang and Qiu 2011; Bruhn and Gerard, 1996). Enhanced DOC levels were often observed at relatively low temperatures (10-20°C) (Yoshika et al., 2002; Mostofa et al., 2005; Fu et al., 2010). Such issues are primarily responsible for the high DOC growth in October compared to July. Conversely, the DOC reached a minimum at midnight (15% and 63% decrease compared to the highest levels observed in July and Oct, respectively) that could be definitely caused by dark/microbial respiration. These processes could ultimately release either gaseous CO_2 or DIC in lake water, thereby representing a significant CO_2 emission source to the atmosphere (Wang et al., 2020; Sobek et al., 2005; Wang et al., 2011). Many studies have reported that in the typical diel vertical migration (DVM) behavior, zooplankton mostly remains in the upper strata during the night and migrates toward colder and darker layers during the day (Wetzel, 2001; Hansson et al. 2007; Li et al., 2020; Etilé et al. 2015). Such DVM trend on community structure and vertical distribution could represent an attempt at escaping from daytime enhanced high sunlight intensity (Cohen and Forward, 2009; Hansson et al. 2007; Karpowicz and Ejsmont-Karabin, 2018; Karpowicz et al., 2019) and from the associated oxidative stress or photoinhibition that may produce high contents of the reactive oxygen species (e.g. $O_2^{\bullet-}$, H_2O_2 and $^{\bullet}OH$) (Cooper and Zika, 1983; Mostofa and Sakugawa, 2009, 2016; Vione

et al., 2006). Note that total respiration in a lake includes the respiration of both photosynthetic organisms (phytoplankton, alga) and heterotrophic organisms (zooplankton, bacteria, benthic invertebrates) that consume the former (Cole et al., 2000). Note also that common productivity analyses use respiration measurements made at night as a constant, to estimate respiration during the day (Portielje et al., 1996). However, it has been reported that microbial/dark respiration increases exponentially with increasing temperature (Hancke and Glud, 2004), and also that heterotrophic bacteria are responsible for most of respiration (> 95%) in the ocean (del Giorgo and Duarte, 2002), half of which (approximately 37 Gt of C per year) takes place in the euphotic layer (del Giorgio and Williams, 2005). Therefore, the highest level of DOC mineralization observed at midnight in this study could definitely derive from microbial degradation. A conceptual model was developed depicting all diurnal changes during July and October, based on the observed results (Fig. 10). These results would thus indicate that high SI, WT and AT or GW would accelerate the complete transformation of autochthonous FDOM into LMW DOM and other mineralization end-products on a 24-h diurnal cycle. Such a behavior could be further increased by the influence of future GW. Indeed, the mentioned changes can be reasonably expected to occur in the future on the basis of increasing water temperature, extended summer season and increased water stratification in response to a predicted GW ranging from 1.5 to 2.0°C (Huisman et al., 2006; Watanabe et al., 2011; Rogelj et al., 2019). Higher temperatures in the tropical zone may additionally accelerate bacterial metabolism, causing a larger fraction of incoming organic carbon to be respired (Tranvik et al., 2009). A recent study of DOC concentrations in over 7500 lakes in six continents suggests that the DOC export is potentially enhanced by global warming in aquatic ecosystems (Sobek et al., 2007).

In essence, rapid diurnal mineralization of HMW FDOM components under conditions of high WT can be related to a further rapid mineralization of DOC and nutrients (Fig. 6), which would subsequently impact on biogeochemical functions and processes, including C, N and nutrient cycling. These effects are expected to have an ultimate impact on trophic levels of water ecosystems as a whole, which could represent a crucial indicator of the potential GW implications for surface-water ecosystems. Finally, the complete mineralization of FDOM that involves about 15% DOC in aquatic ecosystems under conditions of high water temperature can be used as a useful indicator, to predict the potential impacts of GW on surface-water environments. The net daytime contribution of DOC photo-degradation remains however

unresolved because of its decoupling from enhanced DOC from photorespiration, and it should be the focus for further study.

5. Conclusions

It is well-known that the occurrence of phytoplankton induces a continuous release of both EPS and FDOM, due to both photoinduced processes and microbial respiration (Wang et al., 2017; Shammi et al. 2017a, 2017b, 2017c; Guidi et al., 2016; Parlanti et al., 2000; Zhang et al., 2009; Mostofa et al. 2013; Yamashita and Youhei, 2004). FDOM is then subject to continuous sunlight-induced degradation in the upper layer of sunlit surface waters (from 0 to about 5 m, and sometimes even deeper if water is particularly transparent), and to microbial degradation in the lower depths (Amon and Benner, 1994; Moran et al., 2000; Mostofa et al., 2007; Diaz et al., 2013; Amon and Benner, 1996; Mostofa et al., 2005).

In this work, the occurrence in lake waters has been ascertained of different types of autochthonous FDOM that can be produced by phytoplankton, which include EPS, AHLS of C- and M-types, PLS, newly-released PLS, TLS, a combined form of C- and M-types of AHLS, a combined form of TYLS and PALS, as well as their degradation products. The generation of different FDOM components appears to be strictly related to various factors including diurnal and seasonal temperature changes, timescale, type and nature of primary producers, *e.g.* phytoplankton, as well as lake conditions and ambient environment. Further, depending on these environmental factors and conditions, the sequential production of FDOM and its subsequent degradation happens to occur rapidly even in the one-day timeframe.

The information provided in this paper on the continuous production and concurrent degradation processes of FDOM in the aquatic environment are crucial for predicting and evaluating their intensification in the future, due to the expected extended summer seasons caused by increased air and water temperatures and enhanced water stratification, as a consequence of GW. Further, the information presented on the end-products of these processes appear to be of ultimate impact for a better understanding of trophic levels and of most other

biogeochemical processes and functions that occur in aquatic ecosystems as a whole, including the sustainability of the microbial food web and the cycling of C, N and other nutrients. Further studies are warranted to ascertain the types of aquatic microorganisms along with their biogeochemical linkages to FDOM and nutrients in these two lakes.

Author contributions

K.M.G.M. designed the study. Y.L., M.M., X.Y., X.L. and L.L. performed field work, sample preparation, and EEM measurement. Y.L. performed nutrients and other measurements. Y.L. and J.Y. performed PARAFAC analysis. F.-J.Y. and S.L. performed dual NO_3^- isotopes measurement. B.W. performed microscopic phytoplankton measurement. R.M.E., D.V., C.Q.L. and S.-L.L. revised the manuscript. K.M.G.M., N.S. and Y.L. wrote the manuscript.

ACKNOWLEDGMENTS

This work was financially supported by the National Key R & D Program of China (2016YFA0601000) and National Natural Science Foundation of China (U1612441) and also by the Key Construction Program of the National "985" Project, Tianjin University, China.

Notes

The authors declare no competing financial interest.

References

Abboudi, M., Surget, S., Rontani, J.-F., Sempéré, R., Joux, F., 2008. Physiological alteration of the marine Bacterium *Vibrio angustum* S14 exposed to simulated sunlight during growth. Curr. Microbiol. 57, 412-41

Amon, R.M.W., Benner, R., 1994. Rapid cycling of high-molecular-weight dissolved organic matter in the ocean. Nature 369 (6481), 549-552.

Amon, R.M.W., Benner, R., 1996. Photochemical and microbial consumption of dissolved organic carbon and dissolved oxygen in the Amazon River system. Geochim. Cosmochim. Acta 60 (10), 1783-1792.

Andersson, C.A., Bro, R., 2000. The N-way toolbox for MATLAB. Chemom. Intel. Lab. Syst. 52 (1), 1-4.

Beardall, J., 1989. Photosynthesis and photorespiration in marine-phytoplankton. Aquat. Bot. 34, 105–130.

Bruhn, J., Gerard, V.A., 1996. Photoinhibition and recovery of the kelp *Laminaria saccharina* at optimal and superoptimal temperatures. Mar. Biolo. 125, 639-648

Borisover, M., Laor, Y., Parparov, A., Bukhanovsky, N., Lado, M., 2009. Spatial and seasonal patterns of fluorescent organic matter in Lake Kinneret (Sea of Galilee) and its catchment basin. Water Res. 43 (12), 3104-3116.

Cai, W., Liu, J., Zhu, X., Zhang, X., Liu, Y., 2017. Fate of dissolved organic matter and byproducts generated from on-line chemical cleaning with sodium hypochlorite in MBR. Chem. Engineer. J. 323, 233-242

Carpenter, S.R., Cole, J.J., Kitchell, J.F., Pace, M.L., 1998. Impact of dissolved organic carbon, phosphorus, and grazing on phytoplankton biomass and production in experimental lakes. Limnol. Oceanogr. 43, (1), 73-80.

Casareto, B.E., Niraula, M.P., Suzuki, Y., 2012. Dynamics of organic carbon under different inorganic nitrogen levels and phytoplankton composition. Estuar. Coast. Shelf Sci. 102-103 (5), 84-94.

Catalán, N., Marcé, R., Kothawala, D.N., Tranvik, L.J., 2016. Organic carbon decomposition rates controlled by water retention time across inland waters. Nat. Geosci. 9 (7), 501-504.

Coble, P.G., 1996. Characterization of marine and terrestrial DOM in seawater using excitation–emission matrix spectroscopy. Mar. Chem. 51 (4), 325-346.

Coble, P.G., 2007. Marine optical biogeochemistry the chemistry of ocean color. Chem. Rev. 38 (20), 402-418.

Cohen, J.H., Forward, R.B. Jr., 2009. Zooplankton diel vertical migration - a review of proximate control. Oceanogr. Mar. Biol. 47, 77–109.

Cole, J.J., Pace, M.L., Carpenter, S.R., Kitchell, J. F., 2000. Persistence of net heterotrophy in lakes during nutrient addition and food web manipulations. Limnol. Oceanogr. 45, 1718–1730.

Condon, R.H., Steinberg, D.K., Bronk, D., 2010. Production of dissolved organic matter and inorganic nutrients by gelatinous zooplankton in the York River estuary, Chesapeake Bay. J. Plankton Res. 32(2), 153-170.

Cooper W.J., Zika, R.G., 1983. Photochemical formation of hydrogen peroxide in surface and ground waters exposed to sunlight. Science 220, 711.

Cory, R.M., McKnight, D.M., Chin, Y.-P., Miller, P., Jaros, C.L., 2007. Chemical characteristics of fulvic acids from Arctic surface waters Microbial contributions and photochemical

transformations. Geophys. Res. 112 (G4), G04S51.
Cosby, B.J., Hornberger, G.M., Kelly, M.G., 1884. Identification of photosynthesis-light models for aquatic systems II. Application to a macrophyte dominated stream. Ecol. Model. 23, 25-51
Cui H.-Y., Zhang, S.-B., Zhao, M.-Y., Zhao, Y., Wei, Z.-M., 2020. Parallel faction analysis combined with two-dimensional correlation spectroscopy reveal the characteristics of mercury-composting-derived dissolved organic matter interactions. J. Hazard. Mater. 384,121395.
del Giorgo, P.A., Duarte, C.M., 2002. Respiration in the open ocean. Nature 420, 379–384. doi:101038/nature01165
del Giorgio, P.A., Williams, P.J.l.B., 2005. The global significance of respiration in aquatic ecosystems: from single cells to the biosphere. In: del Giorgio PA, Williams P (Eds), *Respiration in aquatic ecosystems*, New York, Academic Press, pp 267–316
Diaz, J.M., Hansel, C.M., Voelker, B.M., Mendes, C.M., Andeer, P.F., Tong, Z., 2013. Widespread production of extracellular superoxide by heterotrophic bacteria. Science 340 (6137), 1223-1226.
Etilé, R.N.D. et al., 2015. Diel Variation of Zooplankton Community Composition, Abundance and Biomass in a West African Tropical Coastal Lagoon (Grand-Lahou, Côte d'Ivoire). Int. J. Agr. Innovat. Res. 3, 1641-1654
Elser, J.J., Chrzanowski, T.H., Sterner, R.W., Schampel, J.H., Foster, J.H., 1995. Elemental ratios and the uptake and release of nutrients by phytoplankton and bacteria in three lakes of the Canadian shield. Microb. Ecol. 29, 145–162.
Farias, J., Rossetti, G.H., Albizzati, E.D., Alfano, O.M., 2007. Solar degradation of formic acid temperature effects on the photo-Fenton reaction. Ind. Eng. Chem. Res. 46, 7580–7586.
Flemming, H.C., Wingender, J., 2010. The biofilm matrix. Nat. Rev. Microbiol. 8 (9), 623-633.
Frölicher, T.L., Fischer, E.M., Gruber, N., 2018. Marine heatwaves under global warming. Nature 560 (7718), 360-364.
Fu. P., Mostofa, K.M.G., Wu, F.C., Liu, C.Q., Li, W., Liao, H., Wang, L., Wang, J., Mei, Y., 2010. Excitation-emission matrix characterization of dissolved organic matter sources in two eutrophic lakes (Southwestern China Plateau). Geochem. J. 44, 99-112
Gao, K., Li, P., Watanabe, T., Walter Helbling, E., 2008. Combined effects of ultraviolet radiation and temperature on morphology, photosynthesis, and DNA of Arthrospira (spirulina) platensis (*Cyanophyta*). J. Phycol. 44, 777-786
Gao, K.L., Ping, Watanabe, T., Walter Helbling, E., 2010. Combined effects of ultraviolet radiation and temperature on morphology, photosynthesis, and DNA of arthrospira (*spirulina*) platensis (*cyanophyta*). Phycology 44 (3), 777-786.
Gligorovski, S., Strekowski, R., Barbati, S., Vione, D., 2015. Environmental Implications of Hydroxyl Radicals (center dot OH). Chem. Rev. 115 (24), 13051-13092.
Grannas, A.M., Martin, C.B., Chin, Y., Platz, M., 2006. Hydroxyl radical production from irradiated Arctic dissolved organic matter. Biogeochemistry 78, 51–66.
Guidi, L., Chaffron, S., Bittner, L., Eveillard, D., Larhlimi, A., Roux, S., Darzi, Y., Audic, S., Berline, L., Brum, J., 2016. Plankton networks driving carbon export in the oligotrophic ocean. Nature 532 (7600), 465-470.
Hagemann, M., et al., 2016. Evolution of photorespiration from cyanobacteria to land plants, considering protein phylogenies and acquisition of carbon concentrating mechanisms. J.

Exper. Bot. 67, 2963–2976
Hansen, A., Kraus, T.E.C., Pellerin, B.A., Fleck, J.A., Bergamaschi, B.A., 2016. Optical properties of dissolved organic matter (DOM) Effects of biological and photolytic degradation. Limnol. Oceanogr. 61 (3), 1015-1032.
Hansson, L.A. et al., 2007. Escape from UV threats in zooplankton: a cocktail of behavior and protective pigmentation. Ecology 88, 1932-1939
Hancke, K., Glud, R.N., 2004. Temperature effects on respiration and photosynthesis in three diatom-dominated benthic communities. Aquat. Microb. Ecol. 37, 265-281. doi:10.3354/ame037265
Helms, J.R., Mao, J., Schmidtrohr, K., Abdulla, H., Mopper, K., 2013. Photochemical flocculation of terrestrial dissolved organic matter and iron. Geochim. Cosmochim. Acta 121 (6), 398-413.
Hoegh-Guldberg, O., Jacob, D., Taylor, M. et al., 2019. The human imperative of stabilizing global climate change at 1.5°C. Science 365, eaaw6974.
Hu, H.J., Wei, Y.X., 2006. The Freshwater Algae of China-Systematics, Taxonomy and Ecology. Science Press, Beijing, China, pp. 1-1023.
Huisman J., Pham Thi, N.N., Karl, D.M., Sommeijer, B., 2006. Reduced mixing generates oscillations and chaos in the oceanic deep chlorophyll maximum. Nature 439, (7074), 322-325.
Hull, V., Parrella, L., Falcucci, M., 2008. Modelling dissolved oxygen dynamics in coastal lagoons. Ecol. Model. 211, 468-480
Jenkinson, H.F., Lappin-Scott, H.M., 2001. Biofilms adhere to stay. Trends Microbiol. 9 (1), 9-10.
Jiang, H., Qiu, B., 2011. Inhibition of photosynthesis by UV-B exposure and its repair in the bloom-forming cyanobacterium *Microcystis aeruginosa*. J. Appl. Phycol. 23, 691-696
Jung, S.W., Youn, S.J., Shin, H.H., Yun, S.M., Ki, J.S., Jin, H.L., 2013. Effect of temperature on changes in size and morphology of the marine diatom, Ditylum brightwellii (West) Grunow (*Bacillariophyceae*). Estuar. Coast. Shelf Sci. 135 (135), 128-136.
Karpowicz, M., Ejsmont-Karabin, J., 2018. Influence of environmental factors on vertical distribution of zooplankton communities in humic lakes. Ann. Limnol. Int. J. Limnol. 54, 17-28.
Karpowicz, M., Ejsmont-Karabin, J., Wiecko, A., Górniak, A., Cudowski, A., 2019. A place in space - the horizontal vs. vertical factors that influence zooplankton (Rotifera, Crustacea) communities in a mesotrophic lake. J. Limnol. 78, 243–258
Koller, M., Salerno, A., Tuffner, P., et al., 2012**.** Characteristics and potential of micro algal cultivation strategies: a review**.** J. Clean. Prod. 37, 377-388
Kothawala, D.N., Murphy, K.R., Stedmon, C.A., Weyhenmeyer, G.A., Tranvik, L.J., 2013. Inner filter correction of dissolved organic matter fluorescence. Limnol. Oceanogr.-Methods 11, 616-630.
Lakowicz, J.R., 2006. Plasmonics in biology and plasmon-controlled fluorescence. Plasmonics 1 (1), 5-33.
Li, G., Gao, K., Gao, G., 2011. Differential impacts of solar UV radiation on photosynthetic carbon fixation from the coastal to offshore surface waters in the South China Sea. Photochem. Photobiol. 87, 329-334
Li, T., et al., 2020. Diel vertical migration of dominant planktonic crustaceans in the south branch of Yangtze Estuary, China. Aquacult. Fish. (accepted).

Liang, X., Xing, T., Li, J., Wang, B., Wang, F., He, C., Hou, L., Li S.-L., 2019. Control of the hydraulic load on nitrous oxide emissions from cascade reservoirs. Environ. Sci. Technol. 53, 11745−11754.

Ma, X., Green, S.A., 2004. Photochemical Transformation of Dissolved Organic Carbon in Lake Superior—An In-situ Experiment. Great Lakes Res. 30, (04), 97-112.

Malinverno, A., Martinez, E.A., 2015. The effect of temperature on organic carbon degradation in marine sediments. Sci. Rep. 5, 17861, doi.org/10.1038/srep17861

Marañón, E., Lorenzo, M.P., Cermeño, P., Mouriñocarballido, B., 2018. Nutrient limitation suppresses the temperature dependence of phytoplankton metabolic rates. The ISME J. 12 (7), 1836-1845.

Matsumoto, K., Hashioka, T., Yamanaka, Y., 2007. Effect of temperature-dependent organic carbon decay on atmospheric pCO_2. J. Geophys. Res. Biogeosci. 112, G02007, doi10.1029/2006JG000187

Mcilvin, M.R., Casciotti, K.L., 2011. Technical updates to the bacterial method for nitrate isotopic analyses. Anal. Chem. 83 (5), 1850-1856.

McKay, G., Rosario-Ortiz, F.L., 2015. Temperature Dependence of the Photochemical Formation of Hydroxyl Radical from Dissolved Organic Matter. Environ. Sci. Technol. 49, 4147−4154.

Mohinuzzaman, M., Yuan, J., Yang, X., Senesi, N., Mostofa, K.M.G., Liu, C.Q., 2020. Insights into solubility of soil humic substances and their fluorescence characterisation in three characteristic soils. Sci. Total Environ. 720, 137395.

Moran, M.A., Sheldon, W., Zepp, R.G., 2000. Carbon loss and optical property changes during long-term photochemical and biological degradation of estuarine dissolved organic matter. Limnol. Oceanogr. 45 (6), 1254-1264.

Mostofa, K.M.G., Yoshioka, T., Konohira, E., Tanoue, E., Hayakawa, K., Takahashi, M., 2005. Three-dimensional fluorescence as a tool for investigating the dynamics of dissolved organic matter in the Lake Biwa watershed. Limnology 6 (2), 101-115.

Mostofa, K.M.G., Yoshioka, T., Konohira, E., Tanoue, E., 2007. Photodegradation of fluorescent dissolved organic matter in river waters. Geochem. J. 41 (5), 323-331.

Mostofa, K.M.G., Wu, F.C., Liu, C.Q., Fang, W.L., Jie, Y., Ying, W.L., Li, W., Mei, Y., 2010. Characterization of Nanming River (southwestern China) sewerage-impacted pollution using an excitation-emission matrix and PARAFAC. Limnology 11 (3), 217-231.

Mostofa, K.M.G., Sakugawa, H., 2009. Spatial and temporal variations and factors controlling the concentrations of hydrogen peroxide and organic peroxides in rivers. Environ. Chem. 6 (6), 524-534.

Mostofa, K.M.G., Yoshioka, T., Mottaleb, A., Vione, D., Eds. Photobiogeochemistry of Organic Matter Principles and Practices in Water Environments, in Environmental Science, Springer, Berlin, Heidelberg, 2013.

Mostofa, K.M.G., Sakugawa, H., 2016. Simultaneous photoinduced generation of Fe^{2+} and H_2O_2 in rivers: An indicator for photo-Fenton reaction. J. Environ. Sci. 47, 34-38.

Mostofa, K.M.G., Jie, Y., Sakugawa, H., Liu, C.-Q., 2019. Equal treatment of different EEM data on PARAFAC modeling produces artifact fluorescent components that have misleading biogeochemical consequences. Environ. Sci. Technol. 53 (2), 561-563.

Parlanti, E., 2000. Dissolved organic matter fluorescence spectroscopy as a tool to estimate biological activity in a coastal zone submitted to anthropogenic inputs. Org. Geochem. 31 (12), 1765-1781.

Parsons, C.T., Rezanezhad, P.F., O'Connell, D.W., Van Cappellen, P., 2017. Sediment phosphorus speciation and mobility under dynamic redox conditions. Biogeosciences 14, 3585–3602.

Perez-Garcia, O., et al., 2011. Heterotrophic cultures of microalgae: Metabolism and potential products. Water Res. 45, 11-36

Portielje, R., Kersting, K., Lijklema, L., 1996. Primary production estimation from continuous oxygen measurements in relation to external nutrient input. Water Res. 30, 625–643.S

Qian, Y., Wang, J., Ren, Z., Li, J. and Guo, Y., 2019. Mapping the increased minimum mortality temperatures in the context of global climate change. Nat. Commun. 10, 4640.

Rogelj, J., Huppmann, D., Krey, V., Riahi, K., Clarke, L., Gidden, M., Nicholls, Z., Meinshausen, M., 2019. A new scenario logic for the Paris Agreement long-term temperature goal. Nature 573 (7774), 357-363.

Segschneider, J., Bendtsen, J., 2013. Temperature-dependent remineralization in a warming ocean increases surface pCO_2 through changes in marine ecosystem composition. Glob. Biogeochem. Cyc. 27 (4), 1214-1225.

Senesi, N., Loffredo, E., The Chemistry of Soil Organic Matter, in Sparks, D.L. (Ed.), Soil Physical Chemistry. CRC Press, Boca Raton, pp. 239–370, 1999.

Shammi, M., Pan, X., Mostofa, K.M.G., Zhang, D., Liu, C.Q., 2017a. Photo−flocculation of algal biofilm extracellular polymeric substances and its transformation into transparent exopolymer particles. Chemical and spectroscopic evidences. Sci. Rep. 7, 9074.

Shammi, M., Pan, X., Mostofa, K.M.G., Zhang, D., Liu, C.Q., Song, W., 2017b. Investigating extracellular polymeric substances from microbial mat upon exposure to sunlight. Poly. Degrad. Stabil. 146, 192-200.

Shammi, M., Pan, X., Mostofa, K.M.G., Zhang, D., Liu, C.Q., 2017c. Seasonal variations and characteristics differences in the fluorescent components of extracellular polymeric substances from mixed biofilms in saline lake. Sci. Bull. 62 (62), 764-766.

Sheng, G.P., Yu, H.Q., 2006. Characterization of extracellular polymeric substances of aerobic and anaerobic sludge using three-dimensional excitation and emission matrix fluorescence spectroscopy. Water Res. 40 (6), 1233-1239.

Sheng, G.P., Yu, H.Q., Li, X.Y., 2010. Extracellular polymeric substances (EPS) of microbial aggregates in biological wastewater treatment systems: A review. Biotechnol. Adv. 28 (6), 882-894.

Sobek, S., Tranvik L.J., Cole J.J., 2005. Temperature independence of carbon dioxide supersaturation in global lakes. Glob. Biogeochem. Cy. 19, GB2003, doi: 10.1029/2004GB002264.

Sobek, S., Tranvik, L.J., Prairie, Y.T., Kortelainen, P., Cole, J.J., 2007. Patterns and regulation of dissolved organic carbon: An analysis of 7,500 widely distributed lakes. Limnol. Oceanogr. 52, 1208–1219

Stedmon, C.A., Markager, S., Bro, R., 2003. Tracing dissolved organic matter in aquatic environments using a new approach to fluorescence spectroscopy. Mar. Chem. 82, 239-254.

Stedmon, C.A., Markager, S., Tranvik, L., Kronberg, L., Slätis, T., Martinsen, W., 2007. Photochemical production of ammonium and transformation of dissolved organic matter in the Baltic Sea. Mar. Chem. 104 (3-4), 227-240.

Sun, H., Liu, H., Han, J., Zhang, X., Cheng, F., Liu, Y., 2018. Chemical cleaning-associated generation of dissolved organic matter and halogenated byproducts in ceramic MBR: Ozone versus hypochlorite. Water Res. 140, 243-250

Tadini, A.M., Nicolodelli, G., Senesi, G.S., Ishida, D.A., Milori, D.M.B.P., 2017. Soil organic matter in podzol horizons of the Amazon region Humification, recalcitrance, and dating. Sci. Total Environ. 613-614C, 160-167.

Tranvik, L.J., Downing, J.A., Cotner, J.B., Loiselle, S.A., Striegl, R.G., Ballatore, T.J., Dillon, P., Finlay, K., Fortino, K., Knoll, L.B., Kortelainen, P.L., Kutser, T., Larsen, S., Laurion, I., Leech, D.M., McCallister, S.L., McKnight, D.M., Melack, J.M., Overholt, E., Porter, J.A., Prairie, Y., Renwick, W.H., Roland, F., Sherman, B.S., Schindler, D.W., Tremblay, S.S.A., Vanni, M.J., Verschoor, A.M., von Wachenfeldt, E., Weyhenmeyer, G.A., 2009. Lakes and reservoirs as regulators of carbon cycling and climate. Limnol. Oceanogr. 54, 2298-2314

Vione, D., Falletti, G., Maurino, V., Minero, C., Pelizzetti, E., Malandrino, M., Ajassa, R., Olariu, R. I., Arsene, C., 2006. Sources and sinks of hydroxyl radicals upon irradiation of natural water samples. Environ. Sci. Technol. 40 (12), 3775-3781.

Wan, D., Sharma, V.K., Liu, L., Zuo, Y., Chen, Y., 2019. Mechanistic insight into the effect of metal ions on photogeneration of reactive species from dissolved organic matter. Environ. Sci. Technol. 53 (10), 5778-5786.

Wan, N., et al., 2015. Cyanobacterial photo-driven mixotrophic metabolism and its advantages for biosynthesis. Front. Chem. Sci. Engineer. 9, 308–316

Wang, F., Wang, B., Liu, C.-Q., Wang, Y., Guan, J., Liu, X., and Yu, Y., 2011. Carbon dioxide emission from surface water in cascade reservoirs–river system on the Maotiao River, southwest of China. Atmos. Environ. 45, 3827-3834

Wang, K., Garg, S., Waite, T.D., 2017. Light-mediated reactive oxygen species generation and iron redox transformations in the presence of exudate from the cyanobacterium *Microcystis aeruginosa*. Environ. Sci. Technol. 51, 8384 – 8395.

Wang, W.-F., et al., 2020. Climatic and anthropogenic regulation of carbon transport and transformation in a karst river-reservoir system. Sci. Total Environ. 707, 135628. doi.org/10.1016/j.scitotenv.2019.135628

Ward, N.D., Keil, R.G., Medeiros, P.M., Brito, D.C., Cunha, A.C., Dittmar, T., Yager, P.L., Krusche, A.V., Richey, J.E., 2013. Degradation of terrestrially derived macromolecules in the Amazon River. Nat. Geosci. 6 (7), 530-533.

Watanabe, S., Sudo, K., Nagashima, T., Takemura, T., Kawase, H., Nozawa, T., 2011. Future projections of surface UV-B in a changing climate. Geophys. Res. Atmos. 2011, 116 (D16).

Wernberg, T., Bennett, S., Babcock, R.C., de Bettignies, T., Cure, K., Depczynski, M., Dufois, F., Fromont, J., Fulton, C.J., Hovey, R.K., Harvey, E.S., Holmes, T.H., Kendrick, G.A., Radford, B., Santana-Garcon, J., Saunders, B.J., Smale, D.A., Thomsen, M.S., Tuckett, C.A., Tuya, F., Vanderklift, M.A., Wilson, S., 2016. Climate-driven regime shift of a temperate marine ecosystem. Science 353 (6295), 169-172.

Weston, N.B., Joye, S.B., 2005. Temperature-driven decoupling of key phases of organic matter degradation in marine sediments. PNAS 102, 17036–17040.

Wetzel, R.G., 2001. Limnology: lake and river ecosystems. San Diego: Academic Press. p. 1006

Whelan, M.E., Rhew, R.C., 2015. Carbonyl sulfide produced by abiotic thermal and photodegradation of soil organic matter from wheat field substrate. J. Geophys. Res. Biogeosci. 120, 54 –62, doi10.1002/2014JG002661

Winter, A.R., Fish, T.A.E., Playle, R.C., Smith, D.S., Curtis, P.J., 2007. Photodegradation of natural organic matter from diverse freshwater sources. Aquat. Toxicol. 84, 215–222

Yamashita, Y., Tanoue, E., 2004. In situ production of chromophoric dissolved organic matter in coastal environments. Geophys. Res. Lett. 31 (14), L14302.

Yamashita, Y., Tanoue, E., 2003. Chemical characterization of protein-like fluorophores in DOM in relation to aromatic amino acids. Mar. Chem. 82 (3-4), 255-271.

Yang, M., Shi, J., Wang, B., Xiao, J., Li, W., Liu, C.-Q., 2020. Control of Hydraulic Load on Bacterioplankton Diversity in Cascade Hydropower Reservoirs, Southwest China. Microb. Ecol. 80, 537–545.

Ye, S., Zeng, G., Wu, H., Liang, J., Zhang, C., Dai, J., Xiong, W., Song, B., Wu, S., Yu, J., 2019. The effects of activated biochar addition on remediation efficiency of cocomposting with contaminated wetland soil. Resources, Conservation and Recycling 140, 278-285

Yoshioka, T., Ueda, S., Khodzher, T., Bashenkhaeva, N., Korovyakova, I., Sorokovikova, L., Gorbunova L., 2002. Distribution of dissolved organic carbon in Lake Baikal and its watershed. Limnology (2002) 3:159–168

Yue, F.J., Li, S.L., Liu, C.Q., Mostofa, K.M.G., Yoshida, N., Toyoda, S., Wang, S.L., Hattori, S., Liu, X.L., 2018. Spatial variation of nitrogen cycling in a subtropical stratified impoundment in southwest China, elucidated by nitrous oxide isotopomer and nitrate isotopes. Inland Waters. 8 (7505), 1-10.

Yu, H.Q., 2020. Molecular insights into extracellular polymeric substances in activated sludge. Environ. Sci. Technol. 54, 7742−7750.

Zark, M., Dittmar, T., 2018. Universal molecular structures in natural dissolved organic matter. Nat. Commun. 9, (1), 3178.

Zhang, Y., Dijk, M.A., Van Mingliang, L., Guangwei, Z., Boqiang, Q., 2009. The contribution of phytoplankton degradation to chromophoric dissolved organic matter (CDOM) in eutrophic shallow lakes field and experimental evidence. Water Res. 43 (18), 4685-4697.

Zhu, Y., Kieber, D.J., 2018. Wavelength and temperature-dependent apparent quantum yields for photochemical production of carbonyl compounds in the North Pacific Ocean. Environ. Sci. Technol. 52, 1929-1939.

Table 1. Fluorescence EEM peaks wavelengths of the components identified in water samples collected from the Jingye lake on July 5 and October 12 at various sub-diurnal times.

Sampling time	Fluorescence peak (Ex/Em)											
	AHLS C-type		AHLS M-type		EPS				TLS or PLS		Newly-released PLS	
	Peak C	Peak A	Peak M	Peak A	Peak M	Peak A	Peak T	Peak Tuv	Peak T	Peak Tuv	Peak T	Peak Tuv
	(nm)											
Jingye lake (July 5 and 6, 2018)												
6:00 – 9:00					270/394	230/394	230/365	270/365				
10:00 – 15:00	315/418	260/418	305/383	220/383					270/338	225/338	285/357	240/357
16:00 – 20:00	325/430	260/430	300/379	240/379					265/338	220/338	280/351	
21:00 – 1:00	310/449	250/449							275/341	225/341		
2:00 – 6:00					270/400	230/400	270/364	230/364				
Jingye lake (Oct 12 and 13, 2018)												
6:00 – 9:00	310/418	260/418	305/394	220/394			285/352	235/352	265/336	220/336		
10:00 – 15:00	350/418	270/418	295/398	235/398			280/354	230/354	270/324	225/324		
16:00 – 20:00	335/430	265/430	295/382	235/382					270/336	225/336		
22:00 – 0:00	355/418	270/418	310/410	225/410	290/442	240/442	290/366	240/366	270/338	225/338		
2:00 – 6:00	355/430	270/430	315/428	225/428			280/374	230/374	270/336	225/336		

Table 2. Fluorescence EEM peaks wavelengths of the components identified in water samples collected from Jingye and Qingnian lakes in May and June at various sub-diurnal times.

Sampling time	Fluorescence peak (Ex/Em)													
	AHLS C-type		AHLS M-type		A combined form of C- and M-types AHLS				TLS or PLS		Newly-released PLS		TYLS or PALS	
	Peak C (nm)	Peak A	Peak M	Peak A	Peak C	Peak A	Peak M	Peak A	Peak T	Peak Tuv	Peak T	Peak Tuv	Peak T	Peak Tuv
May 2019														
6:00														
Jingye lake	340/449	260/449	300/402	235/402					280/338	225/338				
Qingnian lake	340/459	260/459	300/396	225/396					280/334	225/334				220/313
14:00														
Jingye lake	340/468	260/468	300/389	240/389					280/338	225/338				
Qingnian lake	345/449	270/449	305/416	225/416					280/340	225/340			255,265/321,310,306	220/321
June 2019														
6:00														
Jingye lake	340/449	260/449	305/440	240/440					280/344	225/344				
Qingnian lake	320/458	255/458	305/391	235/391					275/339	225/339	290/346	230/346		
14:00														
Jingye lake	340/449	260/449			290/427	230/427	290/382	230/382	280/337	225/337				
Qingnian lake	335/468	260/468	295/402	235/402					275/327	225/327	285/340	225/340		

Fig. 1. Fluorescence EEM images showing the peaks of fluorescent components identified in diurnal water samples collected from Jingye lake on July 5, 2018. The EEM-PARAFAC model was applied to each of the five sub-diurnal groups (6:00-9:00, 10:00-15:00, 16:00-20:00, 21:00-1:00 and 2:00-6:00) of samples collected every hour, in order to illustrate the changes caused by sunlight-induced and microbial degradation effects. The fluorescence intensity in EEM images is expressed as arbitrary unit (a.u.).

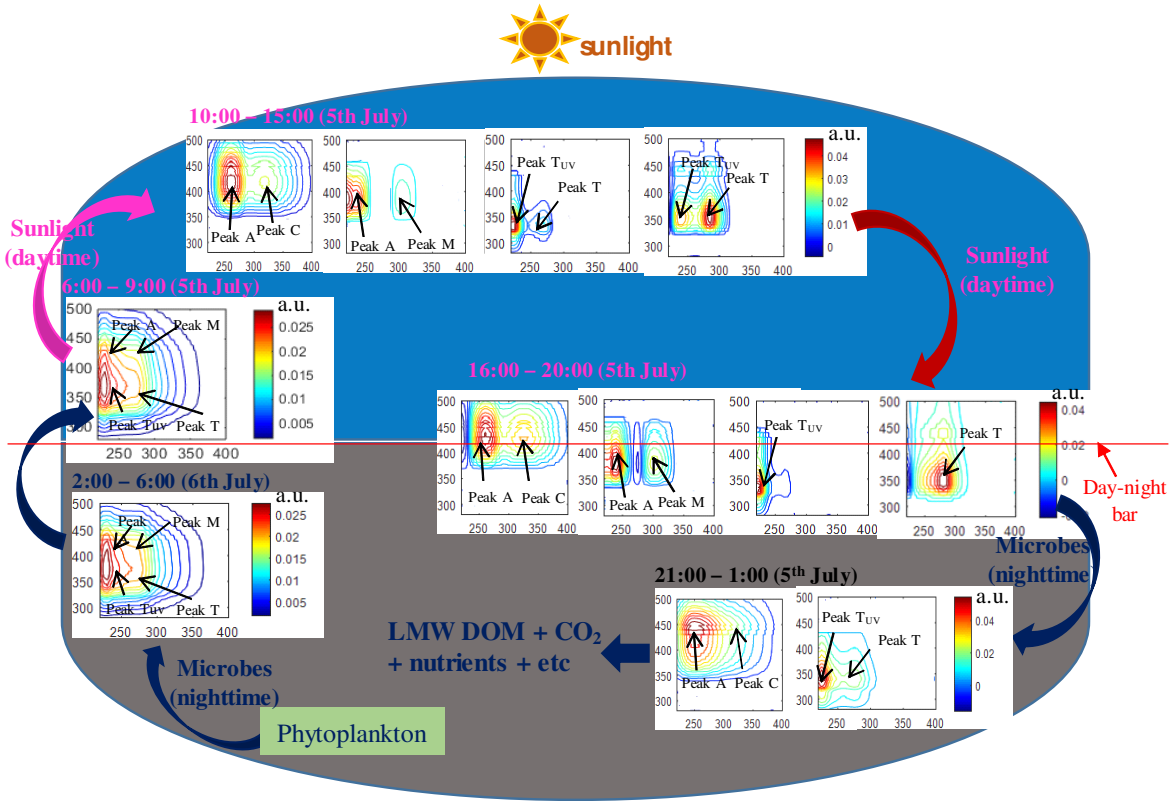

Fig. 2. Variation of air temperature (AT), water temperature (WT) and solar intensity (SI) in the ambient environment of Jingye lake as a function of diurnal sampling time in July 5 and October 12, 2018 (a), and May and June, 2018 (b). Data were provided by Tianjin Meteorological Agency, Tianjin, China.

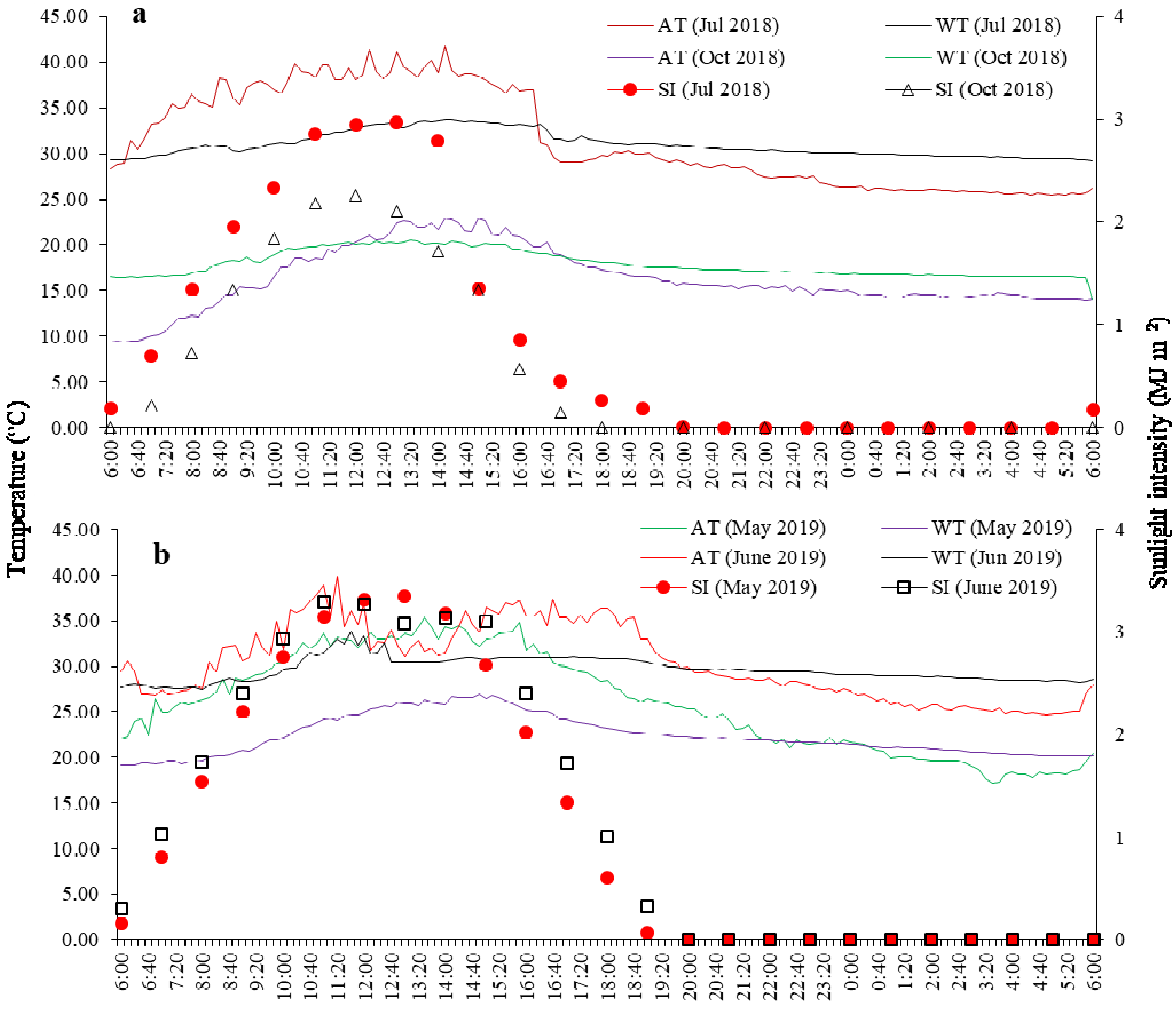

Fig. 3. Fluorescence EEM images showing the peaks of fluorescent components identified in diurnal water samples collected from Jingye lake on Oct. 12 and 13, 2018. The EEM-PARAFAC model was applied individually to each of the five sub-diurnal groups (6:00-9:00, 10:00-15:00, 16:00-20:00, 21:00-1:00 and 2:00-6:00) of samples collected every hour, in order to illustrate the changes caused by sunlight-induced and microbial degradation effects. The fluorescence intensity in EEM images is expressed as arbitrary unit (a.u.).

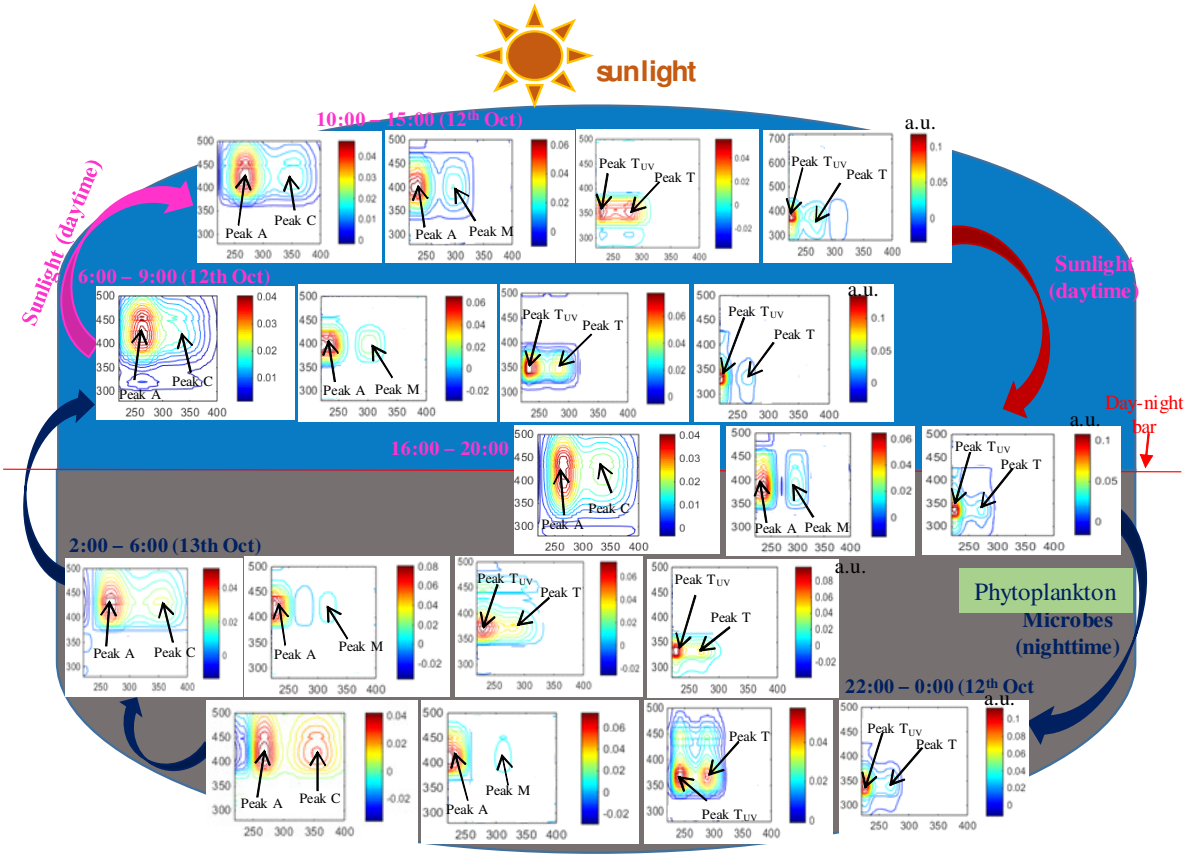

Fig. 4. Fluorescence EEM images showing the peaks of fluorescent components identified in two diurnal (6:00 and 14:00) water samples collected in triplicate from Jingye and Qingnian lakes on June 30, 2019. The EEM-PARAFAC model was applied individually to each of the two sub-sample groups collected at 6:00 and 14:00, in order to illustrate the changes depending on sunlight-induced (14:00) and microbial (6:00) degradation effects. The fluorescence intensity in EEM images is expressed as arbitrary unit (a.u.).

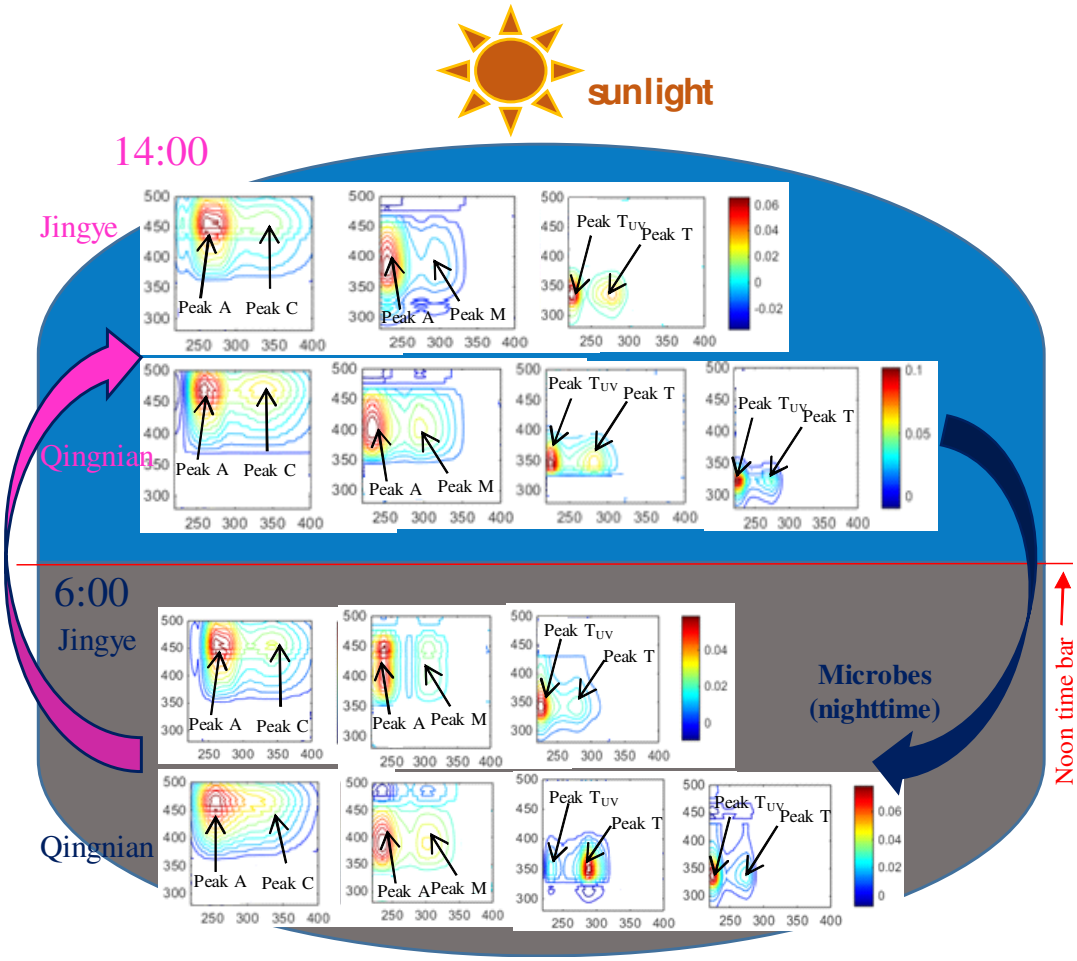

Fig. 5. Fluorescence EEM images showing the peaks of fluorescent components identified in two diurnal (6:00 and 14:00) water samples collected in triplicate from Jingye and Qingnian lakes on May 2, 2019. The EEM-PARAFAC model was applied individually to each of the two sub-sample groups collected at 6:00 and 14:00, in order to illustrate the changes depending on sunlight-induced (14:00) and microbial (6:00) degradation effects. The fluorescence intensity in EEM images is expressed as arbitrary unit (a.u.).

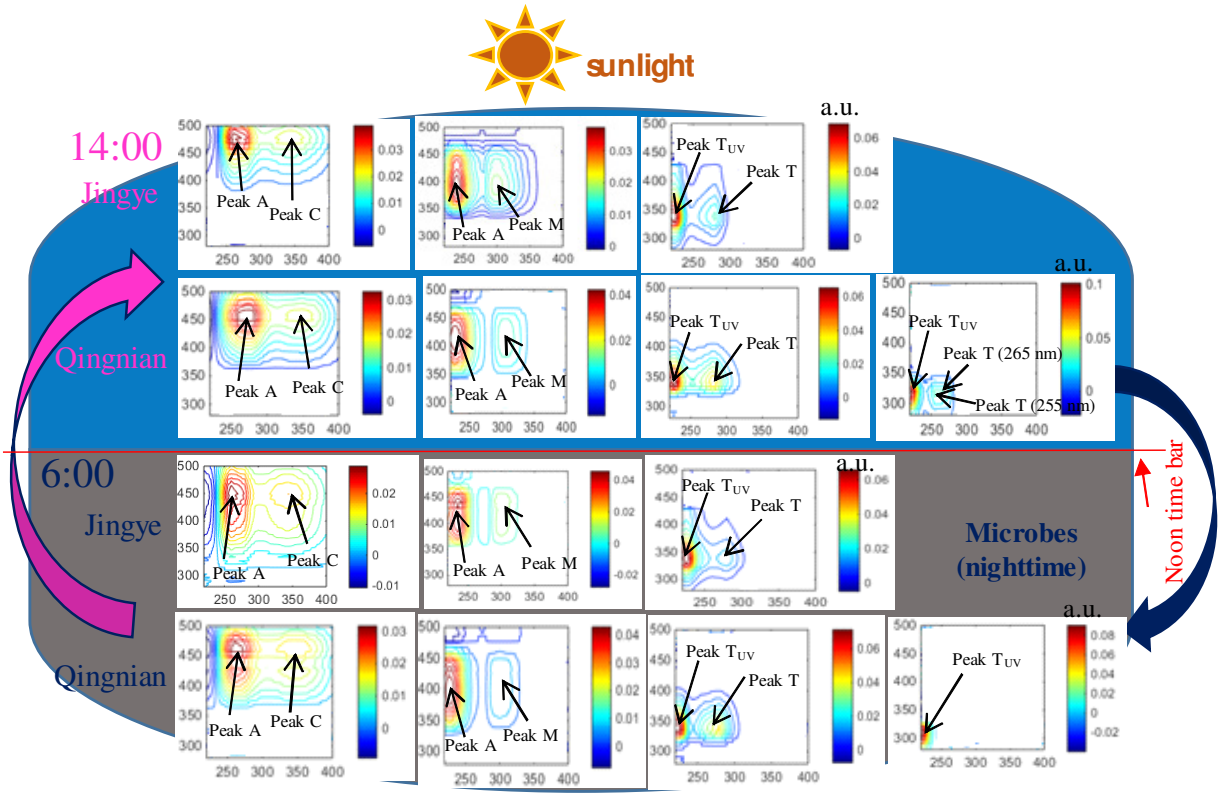

Fig. 6. Changes of nutrient concentrations in diurnal samples from Jingye lake: (a) nitrate (NO_3^-), ammonium (NH_4^+), nitrite (NO_2^-) and dissolved organic nitrogen (DON), and (c) phosphates (PO_4^{3-}) and dissolved silicon (DSi) collected in July; (b) NO_3^-, NH_4^+ and NO_2^- and (d) PO_4^{3-} collected in October; and (e) dissolved organic carbon (DOC) collected in July and October.

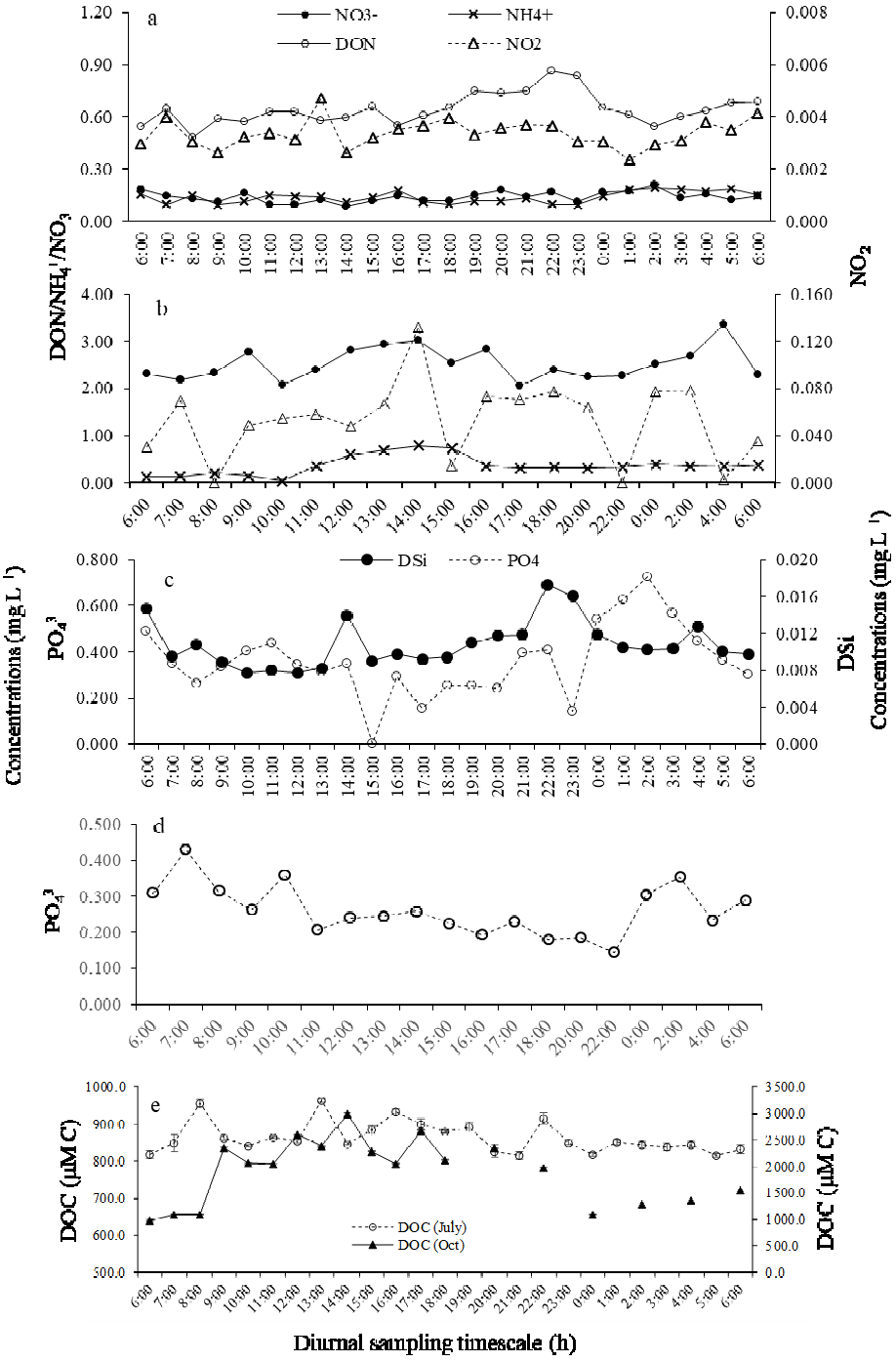

Fig. 7. Flow diagram of the sequential production of autochthonous FDOM from phytoplankton and its subsequent degradation steps until complete mineralization under diurnal conditions as affected by sunlight-induced microbial-induced processes.

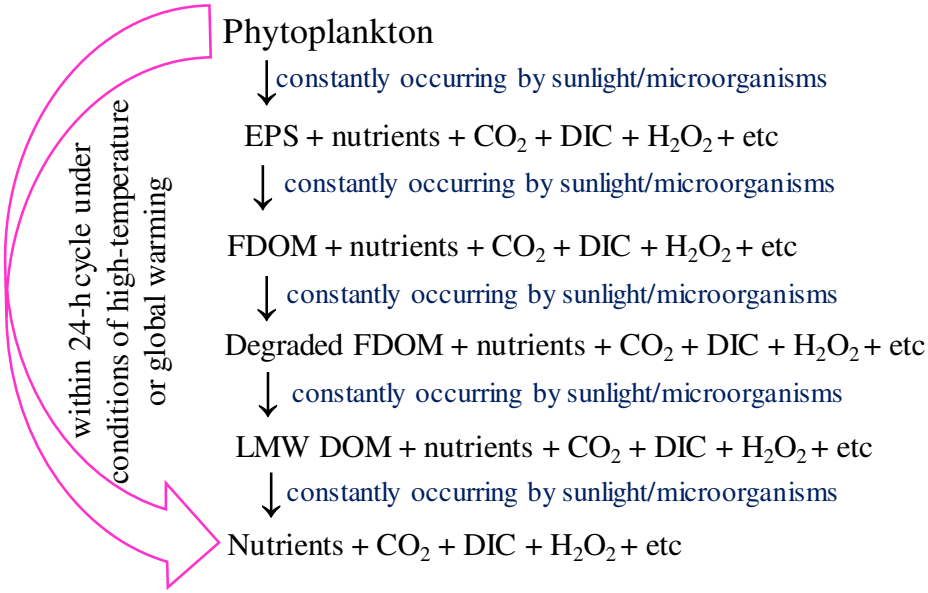

Fig. 8. Pathways of generation and subsequent transformation of EPS into a combined form of C- and M-types HLS that subsequently degrade into individual C-type AHLS and M-type AHLS, which finally degrade to mineralization end-products. The fluorescence intensity in EEM images is expressed as arbitrary unit (a.u.).

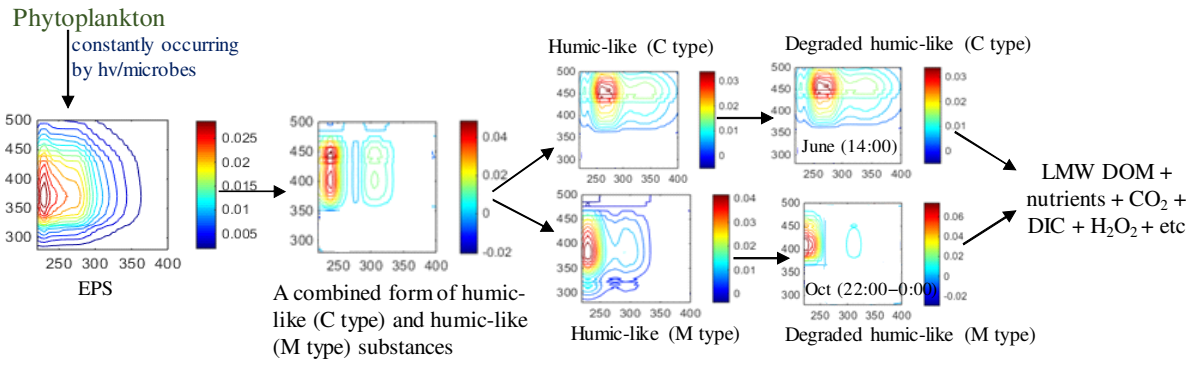

Fig. 9. Pathways of generation and subsequent transformation of EPS into newly-released PLS that then convert into PLS which subsequently generate a combined form of TYLS, PALS and TLS that finally degrade to mineralization end-products. The fluorescence intensity in EEM images is expressed as arbitrary unit (a.u.).

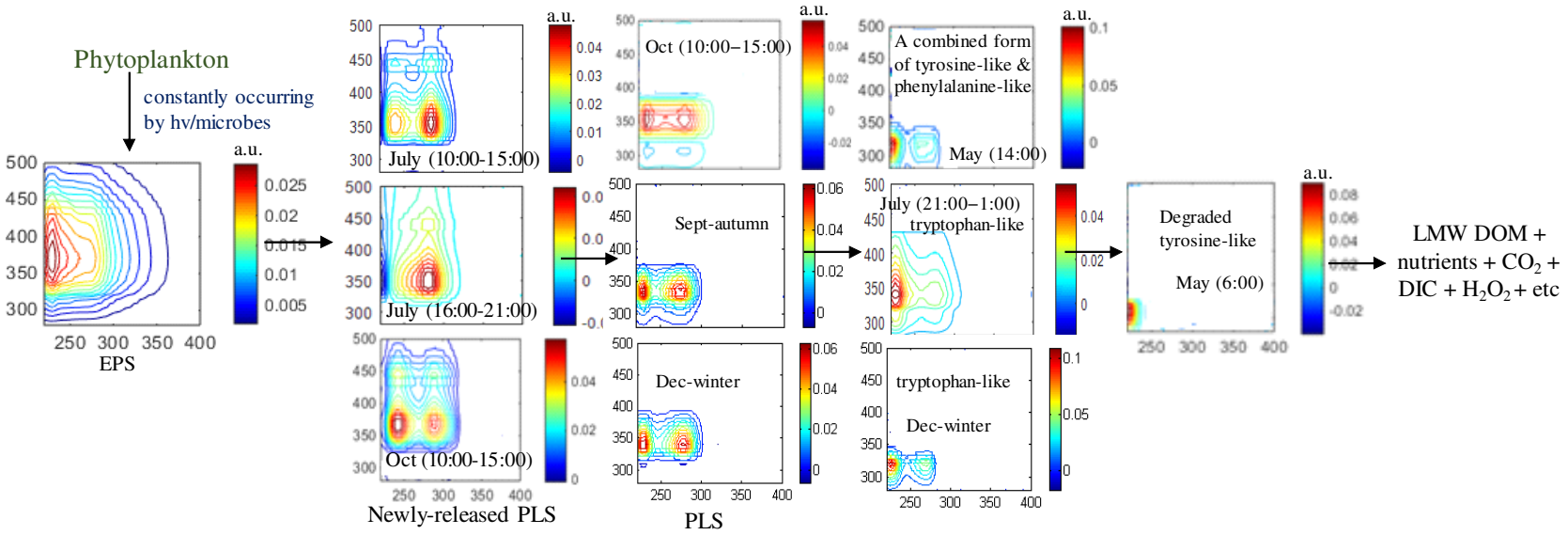

Fig. 10. Natural sunlight can cause the photosynthesis for growth of aquatic organisms along with simultaneous occurrences of photorespiration and photoinhibition depending on the intensity of the sunlight. Photorespiration could produce various fluorescent dissolved organic matter (FDOM) components, nutrients, CO_2, dissolved inorganic carbon (DIC), N_2O and so on, which subsequently undergo daytime photodegradation processes. These all processes could lead to give net dissolved organic carbon (DOC) level in the euphotic zone. The photosynthetically originated microorganisms along with FDOM and nutrients during the nighttime could comprehensively undergo microbial respiration/degradation processes, thereby leading to net changes in DOC, FDOM components and nutrients as a whole.